

FOR FURTHER TRAN

12

AD A055712

NSWC/DL TR-3773

THEORETICAL AND EXPERIMENTAL METHODS IN THE SOLUTION OF MISSILE NONLINEAR ROLL PROBLEMS

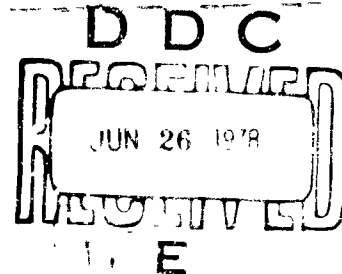
by
PETER DANIELS
SAMUEL R. HARDY
Warfare Analysis Department

JANUARY 1978

Approved for public release; distribution unlimited.

AD No.

DDC FILE COPY



NAVAL SURFACE WEAPONS CENTER

DAHLGREN LABORATORY
Dahlgren, Virginia 22448

WHITE OAK LABORATORY
Silver Spring, Maryland 20910

78 06 12 097

UNCLASSIFIED

SECURITY CLASSIFICATION OF THIS PAGE (When Data Entered)

REPORT DOCUMENTATION PAGE		READ INSTRUCTIONS BEFORE COMPLETING FORM
1. REPORT NUMBER TR-3773	2. GOVT ACCESSION NO.	3. RECIPIENT'S CATALOG NUMBER
4. TITLE (and Subtitle) THEORETICAL AND EXPERIMENTAL METHODS IN THE SOLUTION OF MISSILE NONLINEAR ROLL PROBLEMS,		5. TYPE OF REPORT & PERIOD COVERED
7. AUTHOR(s) Peter/Daniels Samuel R./Hardy		6. PERFORMING ORG. REPORT NUMBER
9. PERFORMING ORGANIZATION NAME AND ADDRESS Naval Surface Weapons Center Dahlgren Laboratory (CK-21) Dahlgren, VA 22448		8. CONTRACT OR GRANT NUMBER(s)
11. CONTROLLING OFFICE NAME AND ADDRESS Naval Surface Weapons Center Dahlgren Laboratory Dahlgren, VA 22448		10. PROGRAM ELEMENT, PROJECT, TASK AREA & WORK UNIT NUMBERS
14. MONITORING AGENCY NAME & ADDRESS (if different from Controlling Office) Naval Air Systems Command Washington, DC 20360		12. REPORT DATE March 1978
		13. NUMBER OF PAGES 66 (12/56p)
		15. SECURITY CLASS. (of this report) UNCLASSIFIED
16. DISTRIBUTION STATEMENT (of this Report) Approved for public release; distribution unlimited.		15a. DECLASSIFICATION/DOWNGRADING SCHEDULE
17. DISTRIBUTION STATEMENT (of the abstract entered in Block 20, if different from Report)		
18. SUPPLEMENTARY NOTES		
19. KEY WORDS (Continue on reverse side if necessary and identify by block number) Missile nonlinear roll Rolling motion theory Roll rate stabilization		
20. ABSTRACT (Continue on reverse side if necessary and identify by block number) This report is a comprehensive documentation of recently developed experimental and theoretical methods dealing with the solution of free flight missile nonlinear roll problems. A unified approach to the development of a nonlinear rolling motion theory for finned missiles as well as a passive roll rate stabilization technique are described.		

DD FORM 1 JAN 73 1473

EDITION OF 1 NOV 65 IS OBSOLETE
S/N 0102-LF-014-6601

UNCLASSIFIED

SECURITY CLASSIFICATION OF THIS PAGE (When Data Entered)

78 06 12 097 341 518

JPL

FOREWORD

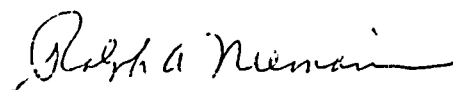
This report describes work directed toward improving the science of free flight missile dynamics by investigating the nonlinear rolling motion phenomena exhibited by finned missiles.

This work was performed under AIRTASK A03W-350D/004B-6F32-300-000.

Acknowledgement is due to W. C. Volz, of the Naval Air Systems Command, who recommended comprehensive documentation of this research.

This report was reviewed by Dr. F. G. Moore, Head, Aeromechanics Branch, and Mr. H. P. Caster, Head, Exterior Ballistics Division.

Released by:



RALPH A. NIEMANN, Head
Warfare Analysis Department

ACCESSION for	
NTIS	White Section <input checked="" type="checkbox"/>
DDC	Bull Section <input type="checkbox"/>
UNANNOUNCED	<input type="checkbox"/>
JUSTIFICATION.....	
BY.....	
DISTRIBUTION/AVAILABILITY CODES	
Dist.	AVAIL. and/or SPECIAL
A	

TABLE OF CONTENTS

	<u>Page</u>
FOREWORD	i
NOMENCLATURE	iii
LIST OF ILLUSTRATIONS	v
LIST OF TABLES	vii
INTRODUCTION	1
LOW DRAG BOMB FLIGHT TRIALS AND NICOLAIDES RESEARCH	1
UNIFIED APPROACH TO A NONLINEAR ROLLING MOTION THEORY . .	5
EXTRACTION OF NONLINEAR ROLL COEFFICIENTS	12
PASSIVE ROLL RATE STABILIZATION	27
ROLL RATE STABILIZED LOW DRAG BOMB	36
PRACTICAL APPLICATION	38
CONCLUSIONS	43
REFERENCES	43
DISTRIBUTION	

NOMENCLATURE

A^*	Planform area of solid fin	in^2
A_F	Planform area of slotted fin	in^2
C_ℓ	Roll moment coefficient	L/QSd
$C_{\ell(\)}$	Roll moment coefficient derivative	$\partial C_\ell / \partial(\)$ rad^{-1}
C_m	Restoring moment coefficient	M/QSd
$C_{m(\)}$	Restoring moment coefficient derivative	$\partial C_m / \partial(\)$ rad^{-1}
C_z	Normal force coefficient	Z/QS
$C_{z(\)}$	Normal force coefficient derivative	$\partial C_z / \partial(\)$ rad^{-1}
d	Reference diameter	ft
I_x	Roll moment of inertia	slug/ft^2
L	Roll moment	ft/lb
M	Restoring moment	ft/lb
γ_T	Roll trim angle	rad
δ	Fin cant angle	rad
ρ	Air density	slug/ft^3
ω_1	Nutation frequency	rad/sec
N	Side moment	ft/lb

$N_{\gamma\alpha}$	Side moment derivative due to roll orientation and angle of attack	ft-lb/rad ²
p	Roll rate	rad/sec
q	Pitching velocity	rad/sec
Q	Dynamic pressure $1/2 \rho V^2$	lb/ft ²
\underline{Q}	Constant	QSd/I_x
S	Reference area	ft ²
V	Total velocity	ft/sec
Z	Normal force	lb
α	Complex angle of attack	rad
α_c	Minimum angle of attack for roll lock-in	rad
γ	Roll orientation angle with respect to the cross component of the total velocity vector	rad

LIST OF ILLUSTRATIONS

<u>Figure</u>	<u>Page</u>
1 Schematic of the Navy Low Drag Bomb (MK 80 Series)	2
2 Characteristic Rolling Motion of Cruciform Finned Missiles With Small Fin Cant	3
3 Schematic of Basic Finner Model	7
4 Induced Rolling Moment vs Roll Orientation Angle for Basic Finner Model Measured in Incompressible Flow	8
5 Induced Rolling Moment Coefficients vs Angle of Attack for Basic Finner in Incompressible Flow	9
6 Hypothetical Damping Function That Can Account for Roll Break Out and Roll Speed Up	10
7 Steady State Spin vs Angle of Attack for the Basic Finner With and Without Fin Cant	11
8 Superposition of Roll Moment Due to Fin Cant on Cubic Damping Function	11
9 Observed Roll Angular Data for Basic Finner Missile at 45° Angle of Attack (Run 1)	13
10 Observed Roll Angular Data for Basic Finner Missile at 45° Angle of Attack (Run 2)	13
11 Comparison of Computed and Observed Roll Angular Data for Basic Finner Missile at 45° Angle of Attack (Run 1)	16
12 Comparison of Computed and Observed Roll Angular Data for Basic Finner Missile at 45° Angle of Attack (Run 2)	16
13 Wrap-Around-Fin Missile Configuration	17
14 Static Roll Moment Coefficient vs Angle of Attack for WAF and Basic Finner Configurations	18
15 Induced Roll Moment Coefficient vs Angle of Attack for WAF and Basic Finner Configurations	18
16 Linear Roll Damping Moment Coefficient vs Angle of Attack for WAF and Basic Finner Configurations	19
17 Cubic Roll Damping Moment Coefficient vs Angle of Attack for WAF and Basic Finner Configurations	19
18 Comparison of Computed and Observed Steady State Roll Rates for WAF Missile Configuration	20

LIST OF ILLUSTRATIONS (Continued)

<u>Figure</u>		<u>Page</u>
19	Schematic of Canard Controlled Missile Configuration	21
20	Extracted Linear Roll Damping Moment Coefficients vs Angle of Attack for Canard Controlled Missile Configurations	22
21	Linear Roll Damping Moment Coefficient Variation With Roll Angle vs Angle of Attack for the Canard Controlled Missile Configurations	23
22	Extracted Induced Roll Moment Coefficient vs Angle of Attack for Canard Controlled Missile Configurations	24
23	Extracted Fin Cant Roll Moment Coefficients vs Angle of Attack for Canard Controlled Missile Configurations	24
24	Extracted Mass/Aerodynamic Roll Moment Asymmetry Coefficients vs Angle of Attack for Canard Controlled Missile Configurations	25
25	Roll Rate vs Dynamic Stability for a Four Fin Missile	27
26	Schematic of Free-Spinning Cruciform Fins	28
27	Rotational Characteristics of Cruciform Rectangular Fins	29
28	Wind Tunnel Model (Naval Academy)	29
29	Steady-State Rolling Velocity vs Angle of Attack for Naval Academy Model With Solid Rectangular Fins. Fin Cant 0.	30
30	Steady-State Rolling Velocity vs Angle of Attack for Naval Academy Model With Solid Rectangular Fins. Fin Cant 8°.	31
31	Steady-State Rolling Velocity vs Angle of Attack for Naval Academy Model With Rectangular Fins and a Slot. $A_F/A^* = 0.691$, $\delta = 0^\circ$	32
32	Steady-State Rolling Velocity vs Angle of Attack for Naval Academy Model With Rectangular Fins and a Small Slot. $A_F/A^* = 0.691$, $\delta = 8^\circ$	32
33	Steady-State Rolling Velocity vs Angle of Attack for Naval Academy Model With Rectangular Fins and a Small Slot. $A_F/A^* = 0.803$	33

LIST OF ILLUSTRATIONS (Continued)

<u>Figure</u>	<u>Page</u>
34 Typical Effect of Slot on Induced Rolling Moment	35
35 Effect of Slot on Amplitude of Induced Rolling Moment	35
36 Schematic of the MK 81 Low Drag Bomb	36
37 WSMR Test Vehicle (MK 82/BSU-49B)	39
38 BSU-49B Fin Planform	39
39 Free Rolling Characteristics of Solid Fin Vehicle	40
40 Free Rolling Characteristics of Slotted Fin Vehicle	40
41 Effects of Fin Configuration on Stability	41
42 Release Envelope and Dynamic Stability Characteristics (WSMR Test Vehicle With 10° Turning Wedges)	42

LIST OF TABLES

<u>Table</u>	<u>Page</u>
1 Aerodynamic Roll Moment Coefficient Considered in Fits	15
2 Flight Conditions and Test Drops for the Standard Low-Drag Bomb and Modified Configuration	37

INTRODUCTION

It had been shown, by the early 1950's,^{1,2,3} that the free-flight dynamic stability of finned missiles depended strongly upon roll rate. The concept of Magnus instability had been developed earlier from the linear theory of missile dynamics, and Nicolaides³ had recently published his important linear theory of simple roll-yaw resonance instability. However, during flight trials of the Navy low drag bomb, an instability occurred that could not be explained by any known roll-yaw coupling theory.

This report summarizes research conducted by the Navy to understand this third type of instability, now known as catastrophic yaw, and provide a solution to this problem.

LOW DRAG BOMB FLIGHT TRIALS AND NICOLAIDES' RESEARCH

The MK 80 series low drag bomb was designed after World War II by the Douglas Aircraft Company and flight-tested at the Naval Proving Ground⁴ (now the Naval Surface Weapons Center, Dahlgren Laboratory). This particular bomb, whose schematic is shown in Figure 1, was fabricated in the 250-lb class (MK 81), 500-lb class (MK 82), 1000-lb class (MK 83), and 2000-lb class (MK 84). It is of interest to note that the MK 82, MK 83, and MK 84 are still fabricated in their original configuration and used extensively by the armed services.

Flight tests at the Naval Proving Ground revealed that the low drag bomb occasionally exhibited a severe instability of the nutation mode that could not be accounted for by the linear theory (i.e., Magnus instability, or resonance instability). Nicolaides' description of this instability cannot be improved upon by these authors, and therefore a direct quote of his description is as follows from Reference 2.

"This particular dynamic instability, when it occurred, was first characterized by the failure of the missile to pick up its full steady state rolling velocity and, then, by a catastrophic growth of the pitching and yawing motion. Initially the rolling velocity increases due to the fin cant. However, when it reaches a value equal to the nutation frequency it holds constant and "locks in" at that particular value instead of seeking the much larger steady state value. Initially the size of the pitching and yawing motion reduces. However, when the rolling motion locks in, it

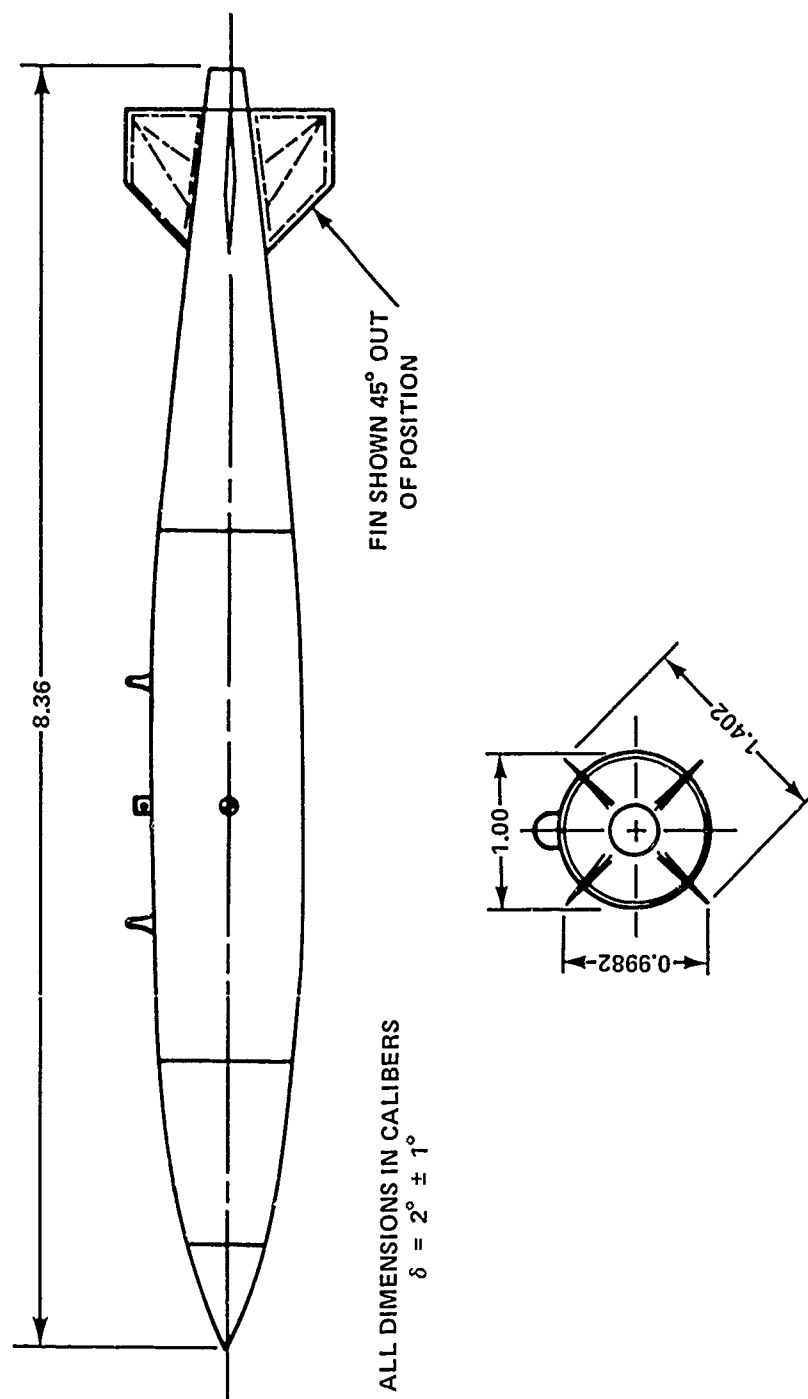


Figure 1. Schematic of the Navy Low Drag Bomb (MK 80 Series)

begins to grow and may very soon reach extreme values such that the missile in flight looks more like a propeller than an arrow. This unique flat spin has been termed 'Catastrophic Yaw.'"

Since the missile's free flight rolling motion was so strongly affected, Nicolaides felt that wind tunnel tests of a free rolling model might be in order. Consequently, he had constructed a sting mounted, free rolling model of the basic finner; a standard Navy research configuration consisting of a cone cylinder body with rectangular fins. Tests were conducted in the National Bureau of Standards wind tunnel.^{5,6,7}

Nicolaides found that four-finned missiles exhibited five separate roll characteristics that he labeled "linear rolling motion," i.e., conforming to the linear theory of missile dynamics, roll "slow down," roll "lock in," roll "break out," and roll "speed up." These roll characteristics depended upon the angle of attack and fin cant and are illustrated in Figure 2.

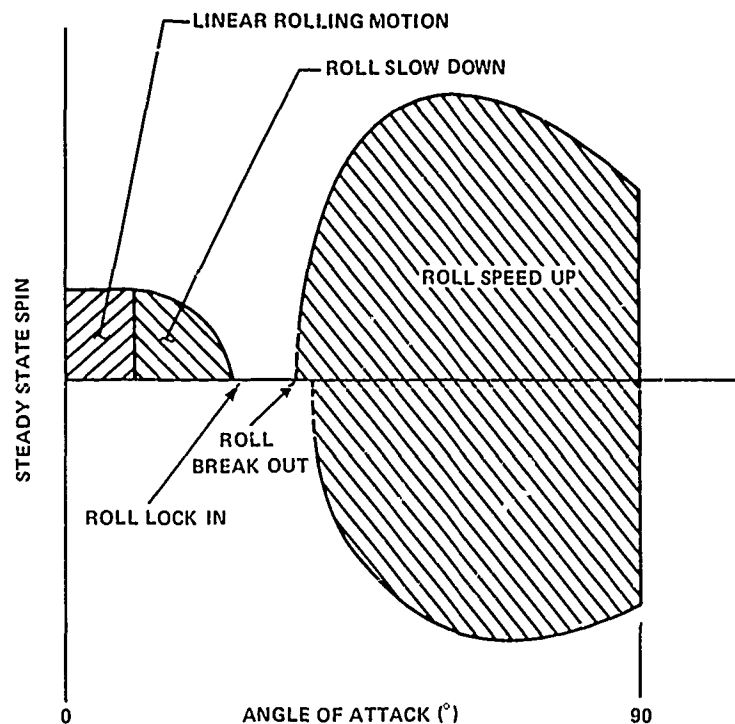


Figure 2. Characteristic Rolling Motion of Cruciform Finned Missiles With Small Fin Cant

In linear rolling motion, near zero yaw, the roll moment is proportional to the fin cant and rolling velocity and is independent of the angle of attack. However, it is found that as the angle of attack increases, the roll rate "slows down" mainly due to a loss in fin cant effectiveness and "locks in;" i.e., the missile fails to roll and exhibits stable oscillations about a roll trim angle (γ_T), tending toward 45° as a limit. At higher angles of attack the missile exhibits unstable oscillation about the roll trim angle and "breaks out," thus developing large roll rates (roll speed up) in either the positive or negative sense, and even against the fin cant moment.

Nicolaides pointed out that the stable oscillations of the model in the "lock in" region suggested the existence of a roll moment that depended upon angle of attack and roll orientation. A literature search revealed that this moment had been measured earlier^{2,8-12} and for a four-finned missile takes the form

$$L(\gamma)\alpha = L_{\gamma\alpha}\alpha \sin 4\gamma \quad (1)$$

The rediscovery of aerodynamic moments with a periodicity of 4γ was the primary factor in explaining the phenomenon of catastrophic yaw.¹³ For an example, consider the flight condition where a four-finned missile has a nutation frequency equal to its rolling velocity. Its roll orientation angle is constant. This unique type of motion is called "lunar" because of its analogy to the motion of the moon. In this free-flight case where δ , α , p , and γ are constant, the rolling equation of motion is

$$L_\delta \delta + L_p p + L_{\gamma\alpha} \alpha \sin 4\gamma = 0 \quad (2)$$

The critical lock in angle of attack (α_C) or the roll trim angle (γ_T) are obtained from Equation (2) as

$$\alpha_C = -(L_\delta \delta + L_p p) / L_{\gamma\alpha} \sin 4\gamma \quad (3)$$

and

$$\gamma_T = \{ \sin^{-1} [-(L_\delta \delta + L_p p) / L_{\gamma\alpha} \alpha] \} / 4 \quad (4)$$

Since γ_T is a constant for this condition, an additional aerodynamic derivative becomes significant. This derivative is known as the induced side moment and can be expressed in the following form for the cruciform finned missile:

$$N(\gamma, \alpha) = N_{\gamma\alpha} \sin 4\gamma \quad (5)$$

The induced side moment acts perpendicular to the plane of the angle of attack and can have a serious destabilizing influence.

The phenomena of roll break out and roll speed up were at first attributed to vortex shedding from the missile body onto the cruciform tail.⁷ However, this theory was abandoned when wind tunnel tests showed that a pure cruciform fin system (no body) exhibited the same nonlinear rolling characteristic, i.e., roll slow down, roll lock in, roll break out, and roll speed up. The nonlinear character of the cruciform fin system suggested that the speed up was induced by vortex shedding from the fins. This experiment has since been verified from at least four different sources.^{26,33}

Nicolaides was unable to develop a nonlinear rolling motion theory to account for roll break out and roll speed up. However, he did suggest that the roll damping moment at high angles of attack was positive at low roll rates in order to account for unstable oscillations about the roll trim point in the break out and speed up regions.²

UNIFIED APPROACH TO A NONLINEAR ROLLING MOTION THEORY

In the early 1960's, it became evident that further research was required in order to design fin stabilized ordnance with satisfactory dynamic stability characteristics at high angles of attack. The problem of roll-yaw coupling instabilities had not been solved for fin span limited ordnance and was particularly acute for fin stabilized, free fall, air launched ordnance ("bombs").

A bomb must be spun in order to average out the effect of aerodynamic asymmetry, usually due to manufacturing tolerances or lugs. If the spin rate approaches the nutation frequency ($p \rightarrow \omega_1$), then resonance oscillations can occur where the trim angle of attack due to asymmetry is amplified to a value inversely

proportional to the total damping in the system.^{1,3} Large coning motion, in excess of that predicted by resonance theory alone, can result if the bomb locks in at the resonance frequency ($p = \omega_1$), whereas large roll rates can trigger Magnus instability.¹

Since bombs can experience large launch disturbances that often result in pitch angles greater than 60° in angle of attack and since the nonlinear character of the roll motion could not be accounted for by the roll equation of motion, dynamic stability analysis of bombs could not be conducted with any degree of confidence.

For example, in the classical linear theory of rolling motion the total aerodynamic roll coefficient for a particular α is

$$C_{\dot{\gamma}}(\delta, p) = C_{\dot{\gamma}_\delta} \delta + C_{\dot{\gamma}_p} p d / (2V) \quad (6)$$

Nicolaides¹³ postulated, and it was later shown² that there existed a periodic (thus, nonlinear) static roll coefficient ($C_{\dot{\gamma}_{4\gamma}} \sin 4\gamma$) which could account for roll lock in. Consequently, the differential equation more recently used¹⁴ to describe the free flight rolling motion of four-finned missiles at a particular α is

$$I_x \dot{p} / Q S d = C_{\dot{\gamma}_\delta}(\alpha) \delta + C_{\dot{\gamma}_p}(\alpha) p d / 2V + C_{\dot{\gamma}_{4\gamma}}(\alpha) \sin 4\gamma \quad (7)$$

For the wind tunnel case with freedom only in roll, $\dot{\gamma} = p$, and Equation (7) may be written as

$$I_x \ddot{\gamma} / Q S d = C_{\dot{\gamma}_\delta}(\alpha) \delta + C_{\dot{\gamma}_\gamma}(\alpha) \dot{\gamma} d / 2V + C_{\dot{\gamma}_{4\gamma}}(\alpha) \sin 4\gamma \quad (8)$$

However, at higher α 's where the lock in becomes unstable and speed up occurs, this approximate equation cannot even qualitatively describe the phenomena.

Consequently, a research study¹⁵ was initiated in an attempt to provide a more accurate mathematical description of single degree of freedom rolling motion. Static and dynamic wind tunnel tests were conducted to provide the information required in order to construct a more exact nonlinear rolling motion theory.

The basic finner (see Figure 3) was tested in the Naval Ship Research and Development Center's 7- X 10-ft subsonic wind tunnel.

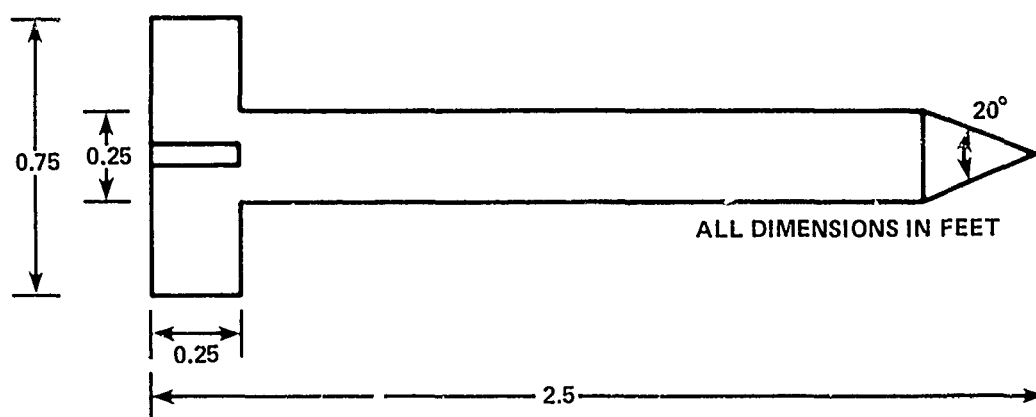


Figure 3. Schematic of Basic Finner Model

The static force data, measured with a strain-gage roll balance, showed that the induced static rolling moment coefficient $C_{\ell}(\gamma)$ is sinusoidal only at very low α 's; at higher α 's, it approaches a more sawtoothed form as illustrated in Figure 4. A least-squares fit of a Fourier sine series was made to the $C_{\ell}(\gamma)$ data for $0 \leq \alpha \leq 90^\circ$. Figure 5 shows the results for the higher-order terms in the series,

$$\sum_{K=1}^4 C_{\ell 4K} \sin 4K\gamma \quad (9)$$

Data obtained at other subsonic velocities show these same characteristics. With these new higher-order terms, Equation (8) becomes

$$I_x \ddot{\gamma} / Q S d = C_{\ell_\delta}(\alpha) \delta + \sum_{K=1}^{\infty} C_{\ell_{4K\gamma}}(\alpha) \sin 4K\gamma + C_{\ell_{\dot{\gamma}}}(\alpha) \dot{\gamma} d / 2V \quad (10)$$

However, Equation (10) still cannot describe the roll break out and roll speed up phenomena.

The dynamic (free roll) tests showed that when the basic finner model is released from rest and allowed to roll freely on a sting mounted, internal, air bearing, it exhibits unstable oscillations about a strong roll trim point at large α 's when the rolling velocity is small, implying that the torque due to roll rate is positive. It then "breaks out" and "speeds up" to a steady-state rate $\ddot{\gamma}_{ss}$, sometime in the direction of, and sometimes opposed to, the cant. At this point the rolling torque as a function of $\dot{\gamma}$ must have a real root with negative slope, since overspinning the missile results in negative damping. It was concluded that if the damping torque is continuous with $\dot{\gamma}$, it must have roughly the cubic form shown in Figure 6.

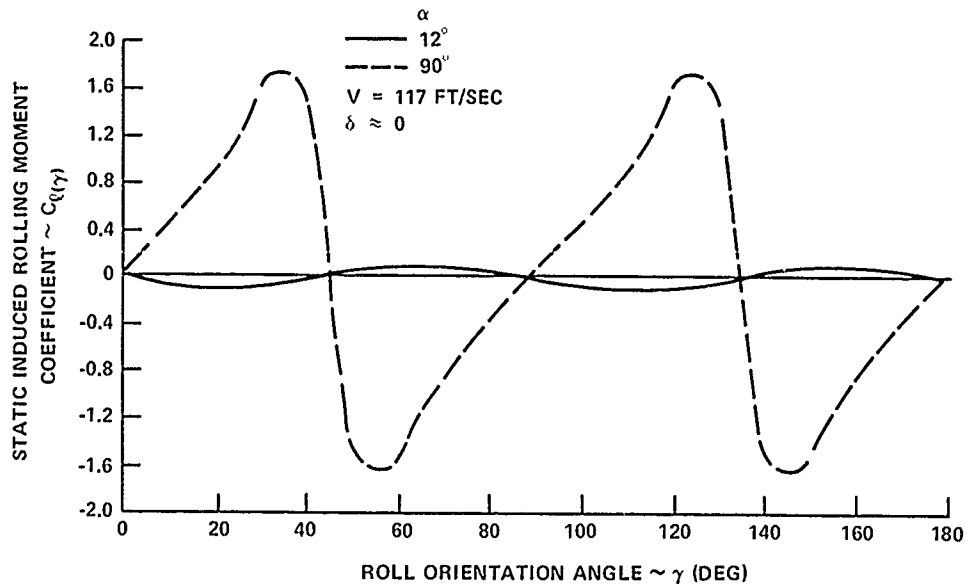


Figure 4. Induced Rolling Moment vs Roll Orientation Angle for Basic Finner Model Measured in Incompressible Flow

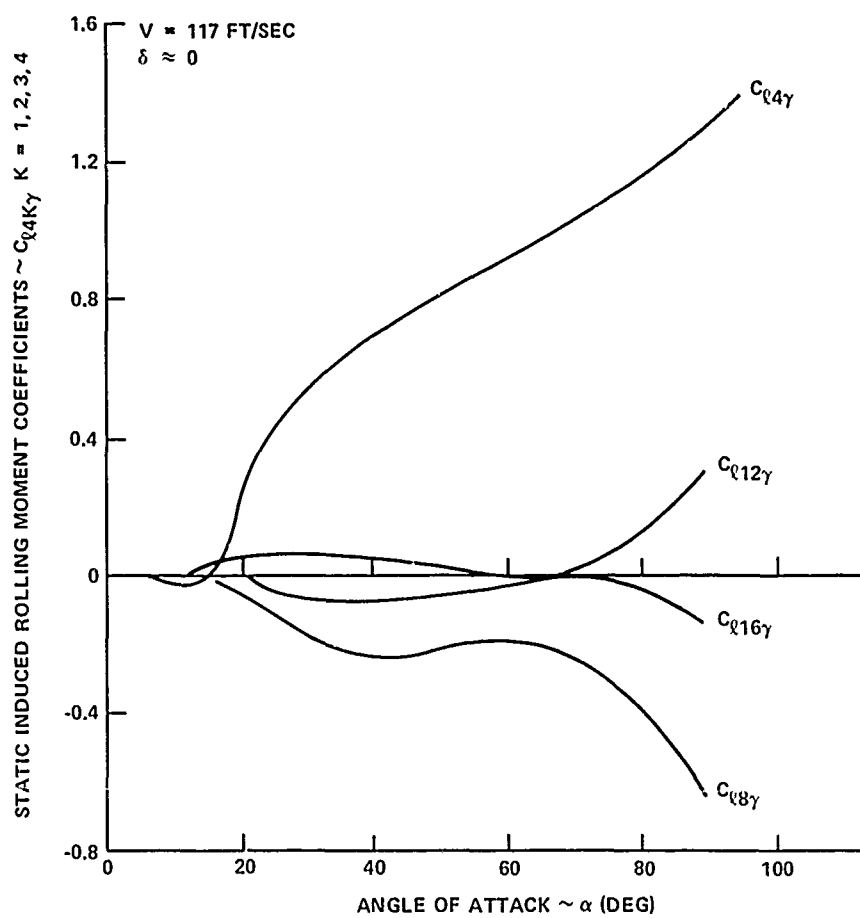


Figure 5. Induced Rolling Moment Coefficients vs Angle of Attack for Basic Finner in Incompressible Flow

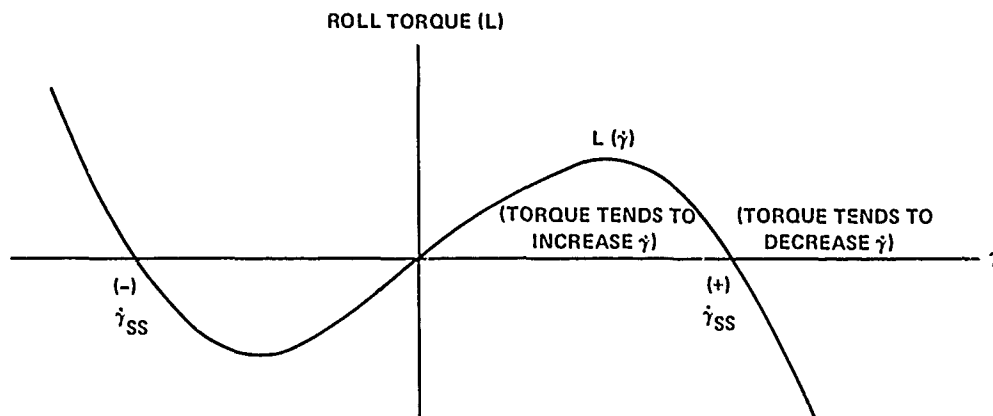


Figure 6. Hypothetical Damping Function That Can Account for Roll Break Out and Roll Speed Up

Figure 7 shows $\ddot{\gamma}_{ss}$ vs α for the basic finner missile with and without fin cant. When $\delta \approx 0$, the dual steady-state spin rates are nearly equal for the particular α . When $\delta \approx 3^\circ$ and in the region of unstable oscillations and break out, there exists a large region where break out is possible only in the positive direction of spin. At slightly higher α 's, where break out can occur in either direction, $\dot{\gamma}_{ss}$ is usually slightly higher in the positive direction of spin.

These rolling characteristics can also be explained in terms of the present nonlinear theory. When the missile is circulating (e.g., $\dot{\gamma}$ does not oscillate) the roll rate approaches a quasi-steady state, and the contribution of the periodic torque may then be neglected. If we then consider a simple superposition of a roll torque due to fin cant ($L_\delta \delta$) on the cubic form of damping as shown in Figure 8, the displacement produces an increase in the positive $\dot{\gamma}_{ss}$ and a decrease in the negative $\dot{\gamma}_{ss}$. Moreover, if the moment due to fin cant is sufficiently large compared to the damping moment, only break out and speed up with positive spin are possible, since the negative spin is damped.

Now if the damping is also analytic with spin, we may express it in the form of a Taylor series whose coefficients depend on odd powers of $\dot{\gamma}$. The Fourier series and Taylor series can be combined into a more general differential equation that contains mixed terms

$$\ddot{\gamma} I_x / (Q S d) = C_{\delta}(\alpha) \delta + \sum_{m,K} C_{\delta m K}(\alpha) \dot{\gamma}^m \sin(4K\gamma + 1/2 m\pi) \quad (11)$$

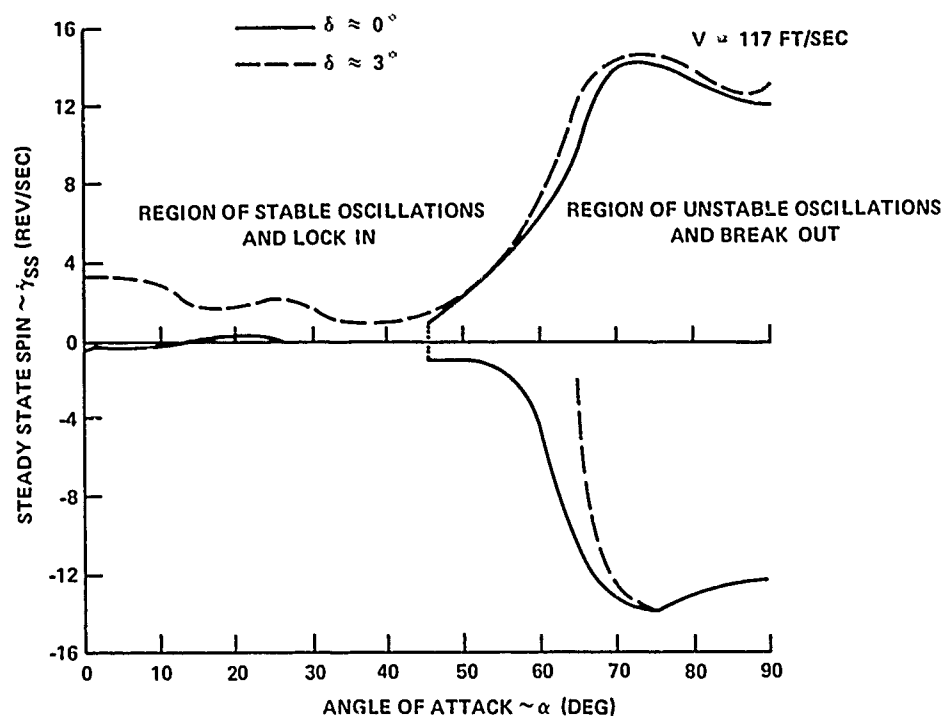


Figure 7. Steady State Spin vs Angle of Attack for the Basic Finner With and Without Fin Cant

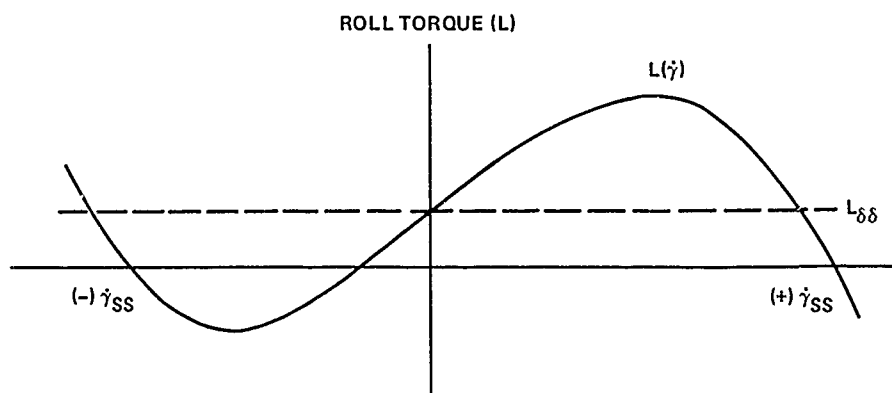


Figure 8. Superposition of Roll Moment Due to Fin Cant on Cubic Damping Function

This is the general form which, when $\delta = 0$, has the symmetry property $\ddot{\gamma}(-\gamma, -\dot{\gamma}) = -\ddot{\gamma}(\gamma, \dot{\gamma})$.

EXTRACTION OF NONLINEAR ROLL COEFFICIENTS

Values for appropriate coefficients are required as a function of angle of attack in order to predict missile roll behavior. High order, nonlinear roll coefficients cannot be readily determined from direct experimental measurement. However, it was found that these coefficients could be determined by fitting Equation (11) to actual observed roll position data.

Observed roll position versus time data were taken from free-rolling subsonic wind tunnel tests.^{15,16} In these tests, the missile was free to roll on a low friction air bearing. The rolling motion history was recorded at selected angles of attack using a motion picture camera. Initial conditions $(\gamma_0, \dot{\gamma}_0)$ were varied at each angle of attack to insure that all modes of the rolling motion were excited. Figures 9 and 10 show two plots of observed data (roll angle (γ) versus frame number) recorded at 45° angle of attack for the basic finner configuration.

Cohen and Clare¹⁷ developed a "global" nonlinear least-squares fitting procedure that could extract roll moment coefficients from observed roll position data. A modified nonlinear least-squares procedure was required for several reasons. The roll behavior is extremely nonlinear in nature. Consequently, a standard nonlinear least-squares fitting technique would require fairly accurate initial estimates of the coefficients in order to begin the fitting process. In general, little is known about the values of the higher-order roll coefficients. Therefore, the fitting process is begun by truncating the equation of motion, thus initially, neglecting higher order terms. In addition, there are further complications due to wind tunnel transients and system noise. As a result, these unmodeled torques can cause the residuals between the computed and observed data to become so large that the process will not converge when the motion is fit continuously.

The "global" nonlinear least-squares procedure allows the observed data to be divided into segments. This procedure provides jumps in roll angle and roll rate between segments, so that the computed data may be restarted in roll regions where the residual would otherwise be too large to allow convergence (of the sum of the squares of the residuals in γ). This "global" process fits the observed data in two

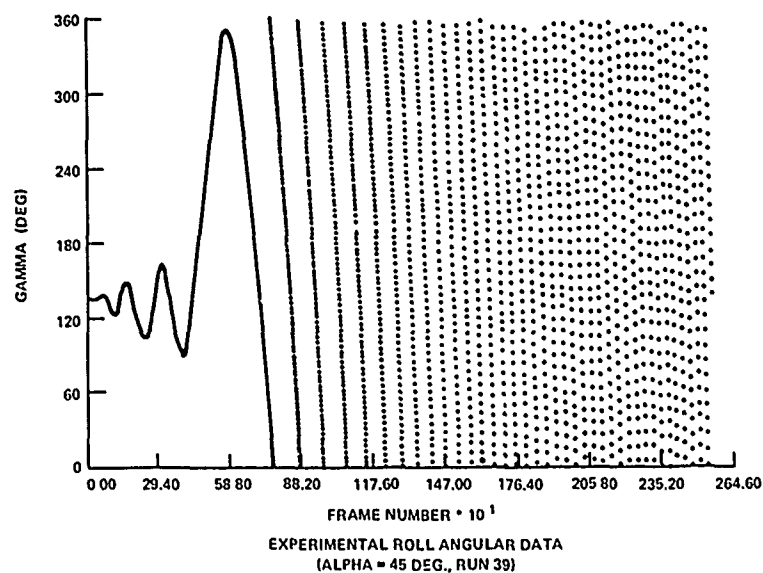


Figure 9. Observed Roll Angular Data for Basic Finner Missile at 45° Angle of Attack (Run 1)

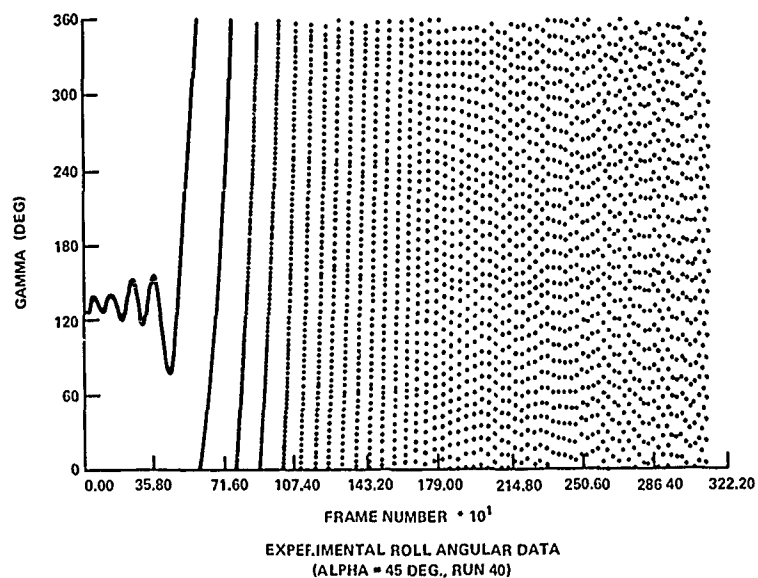


Figure 10. Observed Roll Angular Data for Basic Finner Missile at 45° Angle of Attack (Run 2)

phases. First, each data segment is fit independently ("locally") using constant best-estimate aerodynamic coefficients to determine initial conditions for that segment. Then all of the segments are fit "globally" for a new set of aerodynamic roll moment coefficients and new segment initial conditions.

Cohen and Clare generalized Equation (11) and incorporated it into a computer program to extract roll coefficients. The rewritten equation of motion including mass and/or aerodynamic asymmetry terms is

$$\ddot{\gamma} = Q \sum_{j=0}^J \left(\frac{\dot{\gamma}_d}{2V} \right)^j \sum_{k=0}^K (C_{jk} \cos 4k\gamma + S_{jk} \sin 4k\gamma) + C_{ac} \cos \gamma + C_{as} \sin \gamma \quad (12)$$

where

C_{ac} and C_{as} are the asymmetry terms.

The correspondence between the coefficients used in Equation (12) and more conventional nomenclature is shown in Table 1.

All modes of motion at the same angle of attack are combined and segmented to make up observed roll angular data to be input into the fitting program. Usually only estimates of the basic coefficients are required to begin the fitting process. Once a fit is achieved with the basic coefficients, additional coefficients may be extracted as desired. After the desired set of coefficients are extracted, the segmented lengths are increased to minimize the errors in the extracted coefficient values due to the jumps between segments. The process is usually repeated until a set of coefficients is obtained at each angle of attack. Figures 11 and 12 show typical comparison plots of observed and computed roll angle versus time for the basic finner. The computed data was calculated using the set of extracted roll coefficients for that particular angle of attack and configuration. The small lines drawn normal to the computed data indicate segment locations.

Further details about the procedure are found in Reference 18. Specific details of the computer coding are found in Reference 19.

The technique was first applied to roll position data obtained at subsonic speed for the basic finner configuration at 45, 57, and 66° angle of attack. A set of 14 roll moment coefficients was extracted at each of the three angles of attack. Comparison plots of observed and computed (based on extracted coefficients) roll position data showed excellent agreement. These fits coupled with statistical and

Table 1. Aerodynamic Roll Moment Coefficients
Considered in Fits

Coefficient*		Description
Conventional Nomenclature	Computer Program Nomenclature	
$C_{\ell \delta}$	C_{00}	Fin cant roll moment coefficient
$C_{\ell \delta(4\gamma)}$	C_{01}	Variation of fin cant Moment coefficient With roll angle
$C_{\ell \delta(8\gamma)}$	C_{02}	
$C_{\ell \delta(12\gamma)}$	C_{03}	
\vdots	\vdots	
$C_{\ell \delta(4K\gamma)}$	C_{0K}	
$C_{\ell p}$	C_{10}	Linear roll damping Moment coefficient
$C_{\ell p^2}$	C_{20}	Quadratic roll damping Moment coefficient
$C_{\ell p^3}$	C_{30}	Cubic roll damping moment Coefficient
\vdots	\vdots	
$C_{\ell p^4}$	C_{40}	
$C_{\ell p(4\gamma)}$	C_{11}	Variation of linear roll Damping moment coefficient With roll angle
$C_{\ell p(8\gamma)}$	C_{12}	
$C_{\ell p(12\gamma)}$	C_{13}	
\vdots	\vdots	
$C_{\ell p(4K\gamma)}$	C_{1K}	
$C_{\ell(4\gamma)}$	S_{01}	Induced rolling moment Coefficients
$C_{\ell(8\gamma)}$	S_{02}	
$C_{\ell(12\gamma)}$	S_{03}	
\vdots	\vdots	
$C_{\ell(4K\gamma)}$	S_{0K}	
	C_{ac}	Roll asymmetry coefficients (Combinations of Aerodynamic and mass Asymmetry constants)
	C_{as}	

All coefficients are functions of the missile's angle of attack.

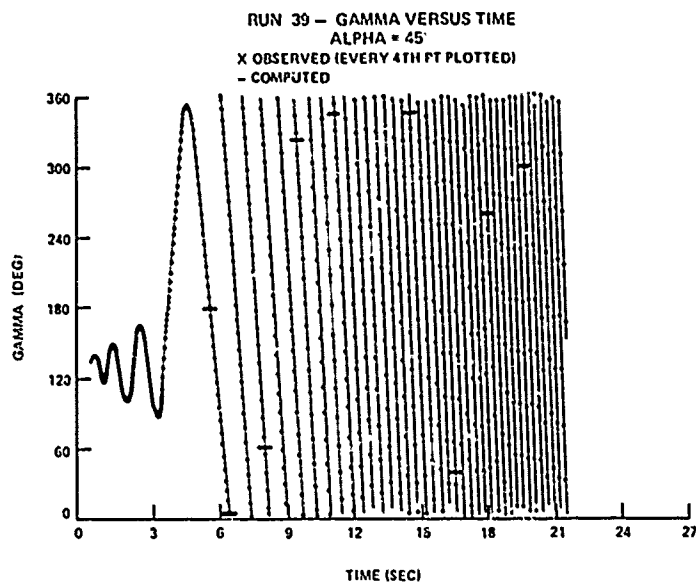


Figure 11. Comparison of Computed and Observed Roll Angular Data for Basic Finner Missile at 45° Angle of Attack (Run 1)

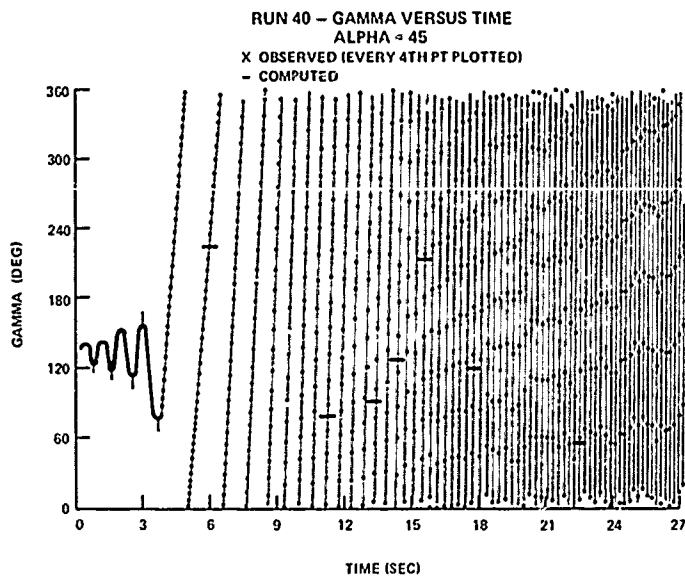


Figure 12. Comparison of Computed and Observed Roll Angular Data for Basic Finner Missile at 45° Angle of Attack (Run 2)

phase plane analysis verified the equation of motion and the extracted coefficients. Reference 18 documents the application of the fitting procedure, the coefficient results, and analysis for the basic finner configuration.

The fitting procedure was later applied to subsonic roll angular data for a wrap-around-fin (WAF) missile configuration, shown in Figure 13, at angles of attack from 0 to 90°. This application extended the utility of Equation (12) to a configuration with 90° rotational symmetry. Figures 14 through 17 show plots of the four basic roll coefficients ($C_{\ell\delta}$, $C_{\ell p}$, $C_{\ell p^2}$, and $C_{\ell(\dot{\gamma})}$) versus angle of attack for the WAF configuration. The corresponding coefficients for the basic finner (a straight finned missile) are also presented for comparison purposes in Figures 14 through 17. The variations of the basic coefficients may be used to explain the roll characteristics of the WAF configuration.

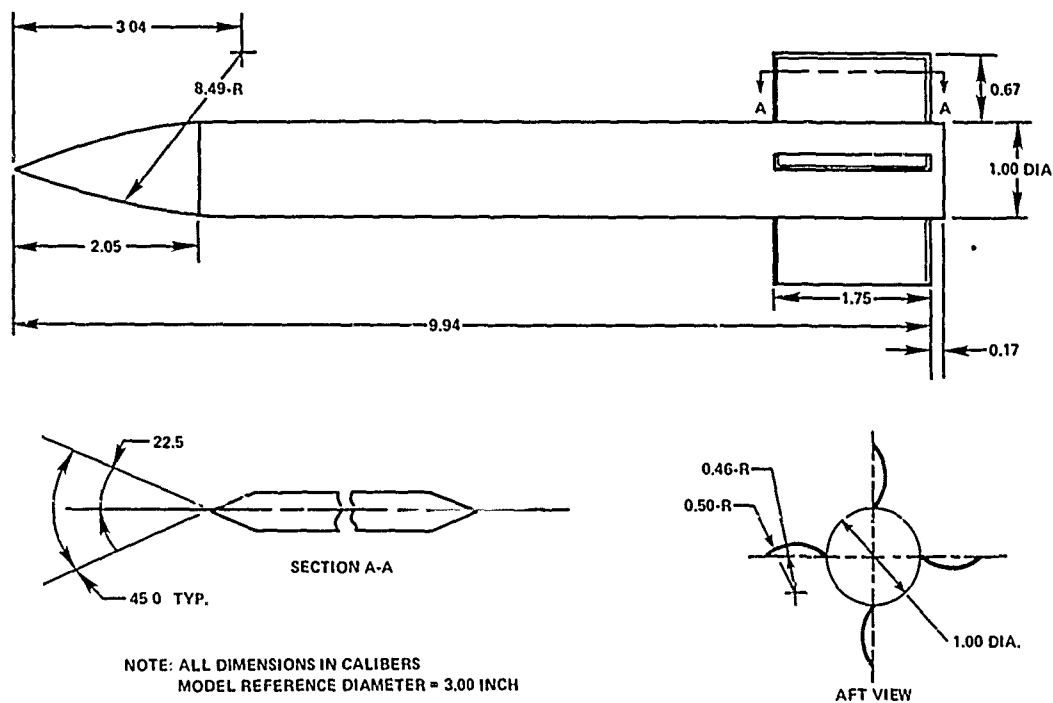


Figure 13. Wrap-Around-Fin Missile Configuration

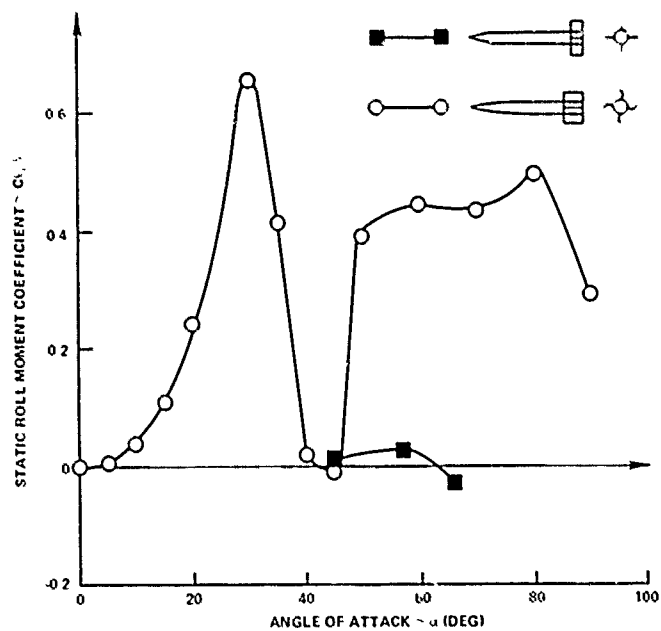


Figure 14. Static Roll Moment Coefficient vs Angle of Attack for WAF and Basic Finner Configurations

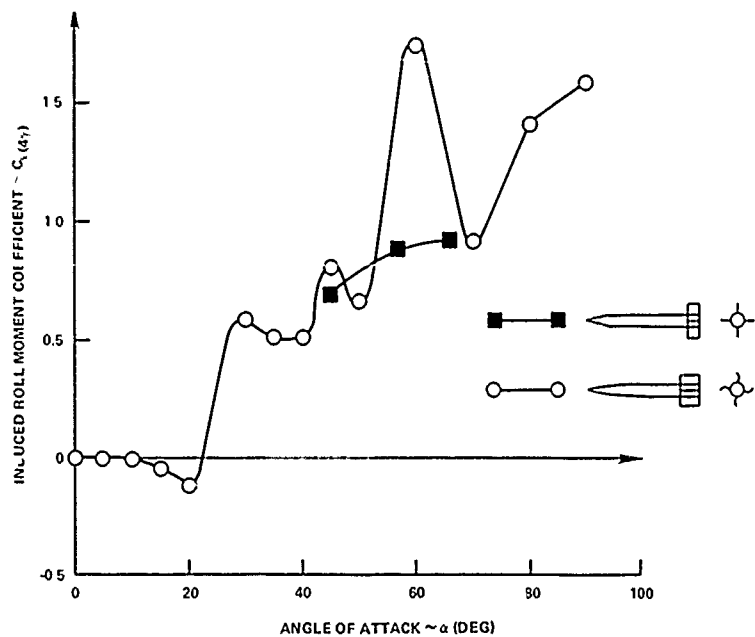


Figure 15. Induced Roll Moment Coefficient vs Angle of Attack for WAF and Basic Finner Configurations

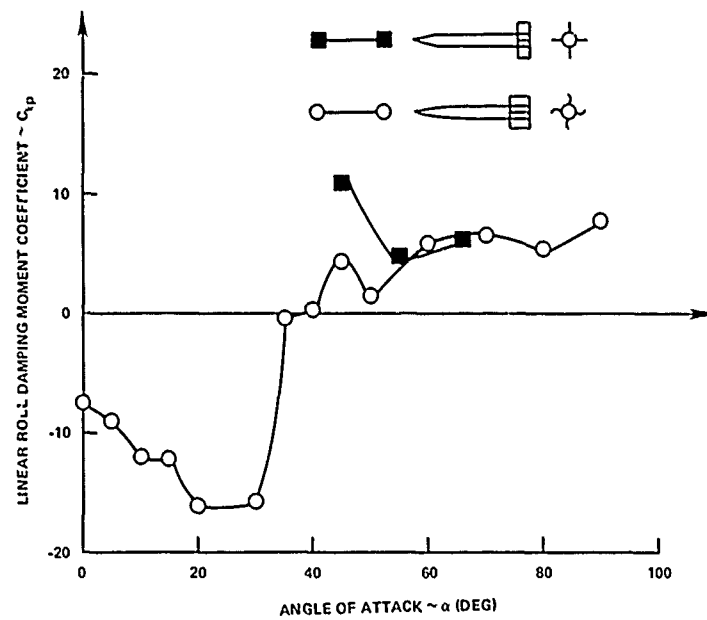


Figure 16. Linear Roll Damping Moment Coefficient vs Angle of Attack for WAF and Basic Finner Configurations

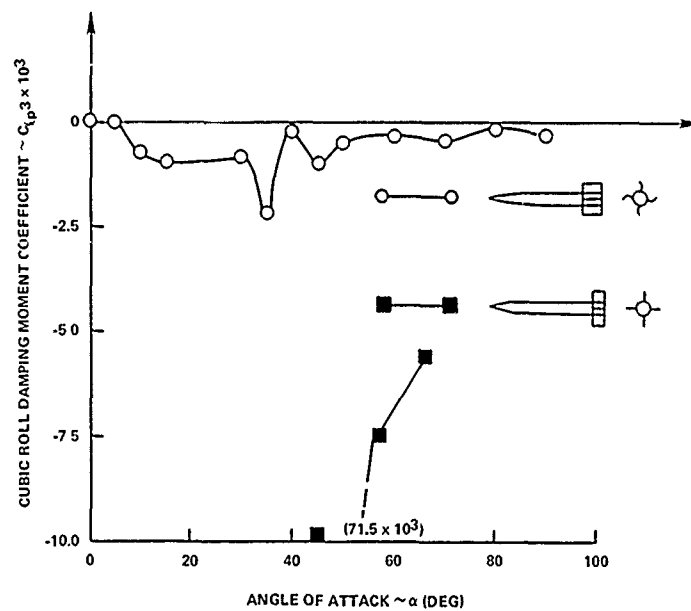


Figure 17. Cubic Roll Damping Moment Coefficient vs Angle of Attack for WAF and Basic Finner Configurations

Figure 18 shows the predicted and observed steady-state roll rates versus angle of attack for the WAF configuration. These predicted rates were calculated using the extracted sets of roll moment coefficients. The principal differences in the roll characteristics between the WAF and straight finned configurations can be seen by comparing Figures 7 and 18. The straight finned configuration has a tendency to develop high roll rates at high angles of attack, in either direction and even against the fin cant, while the WAF configuration has a greater tendency to spin at high rate, in a single direction, at high angles of attack. The major difference in these two types of roll motion is probably due to static roll torque produced by induced drag of the curved fin.²¹

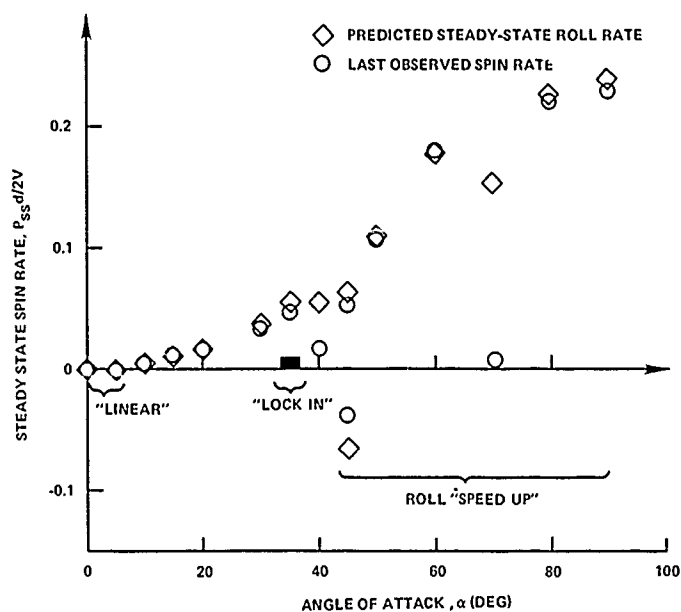


Figure 18. Comparison of Computed and Observed Steady State Roll Rates for WAF Missile Configuration

The effect of WAF curvature is primarily reflected in the static roll moment coefficient. In Figure 14, the WAF static roll moment increases with angle of attack up to 35° ; however, at 40° and 45° , the static roll moment abruptly reduces to zero. Above 45° , large static roll moment is again present. Conversely, a cruciform finned missile with intentional fin cant (δ) would exhibit a static roll moment that decreases with increasing angle of attack as suggested by classical roll slow down.¹⁵

The fitting technique has also been applied to the canard controlled missile configuration^{22,23} shown in Figure 19. Three configurations were tested in order to determine relative contributions of the canard, tail, and canard/tail interference. The buildup configurations included canard + body, body + tail, and canard + body + tail, all with zero fin deflections. In addition, a canard + body + tail configuration with two canards deflected 15° to simulate a pitch control command was tested to determine the change in roll damping due to a large fin deflection.

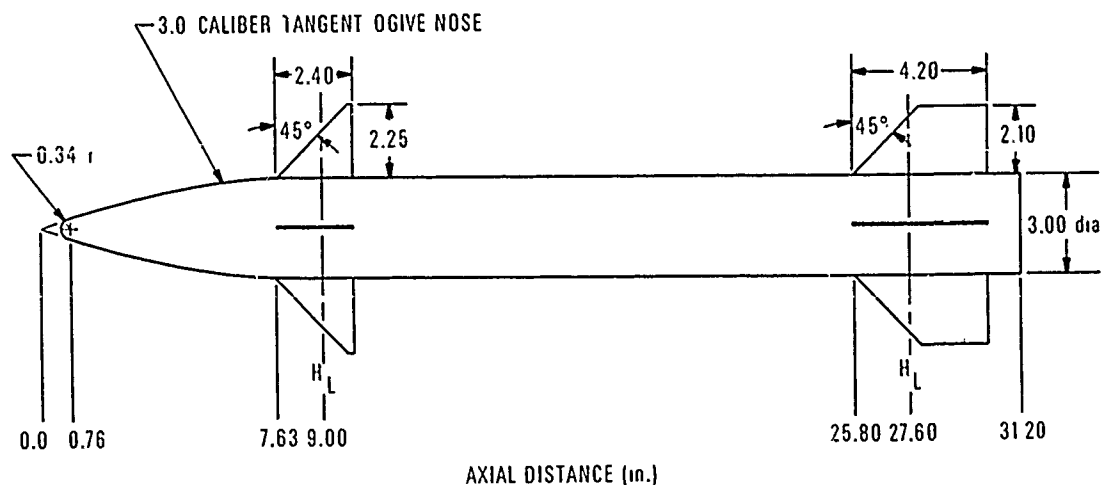


Figure 19. Schematic of Canard Controlled Missile Configuration

In this application only basic roll coefficients were relevant. These included static roll moment ($C_{l\delta}$), linear roll damping (C_{lp}), linear roll damping variation with roll angle ($C_{lp(4\gamma)}$), and induced roll moment coefficients ($C_{l(4\gamma)}$ and $C_{l8\gamma}$). The higher-order coefficients ($C_{lp(4\gamma)}$ and $C_{l8\gamma}$) were included when they made a significant improvement in the data fit. Figures 20 through 24 present plots of the extracted coefficients versus angle of attack for the four configurations.

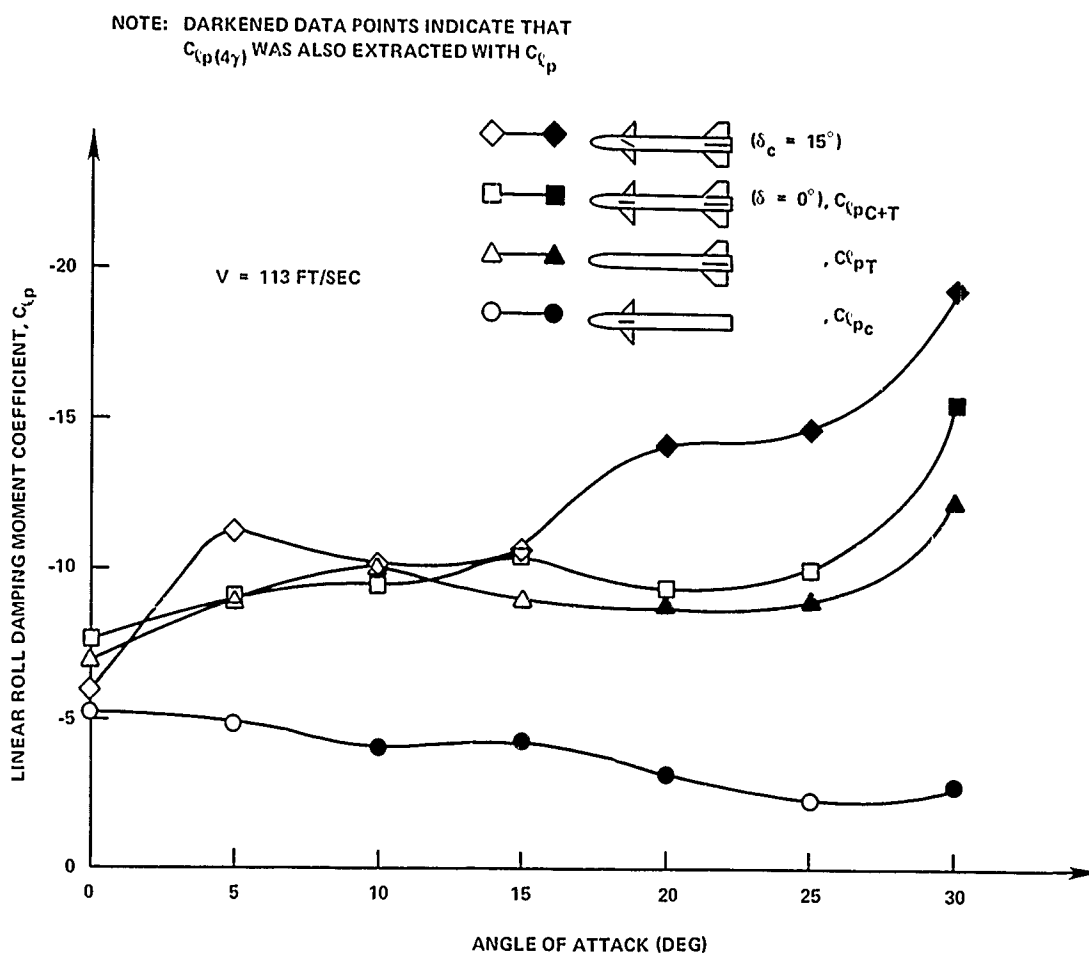


Figure 20. Extracted Linear Roll Damping Moment Coefficients vs Angle of Attack for Canard Controlled Missile Configurations

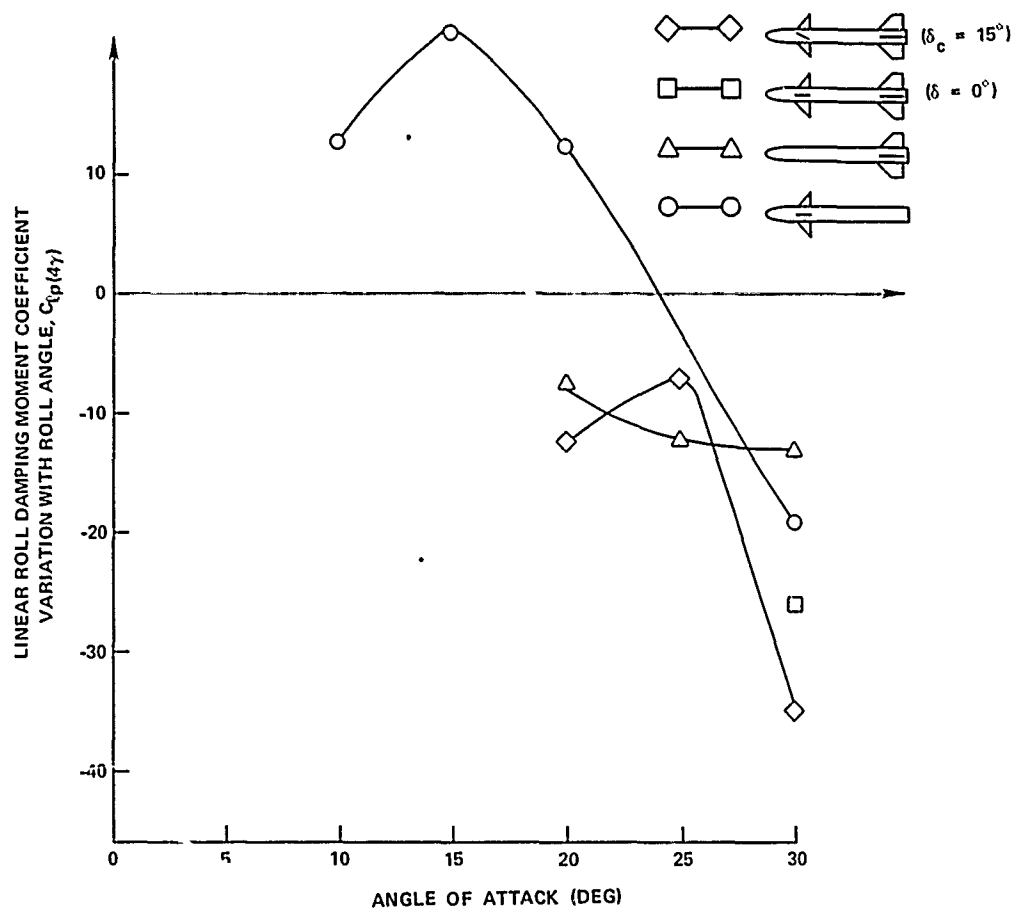


Figure 21. Linear Roll Damping Moment Coefficient Variation With Roll Angle vs Angle of Attack for the Canard Controlled Missile Configurations

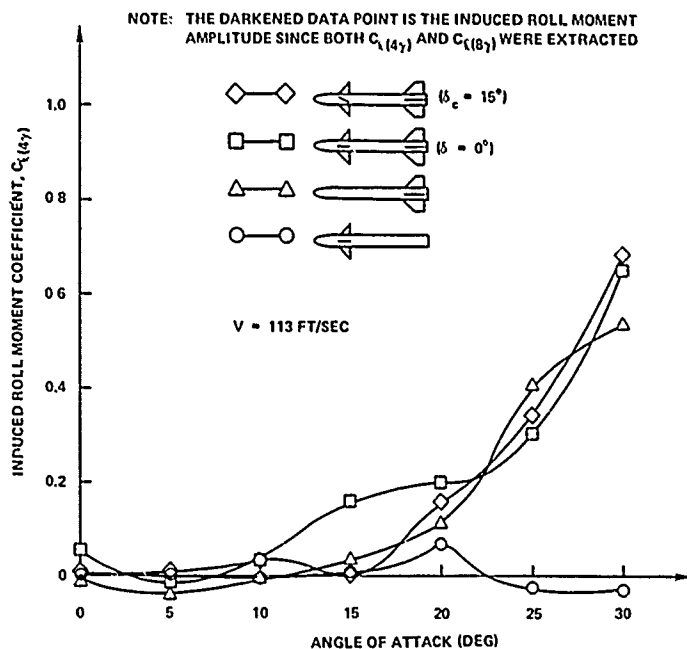


Figure 22. Extracted Induced Roll Moment Coefficient vs Angle of Attack for Canard Controlled Missile Configurations

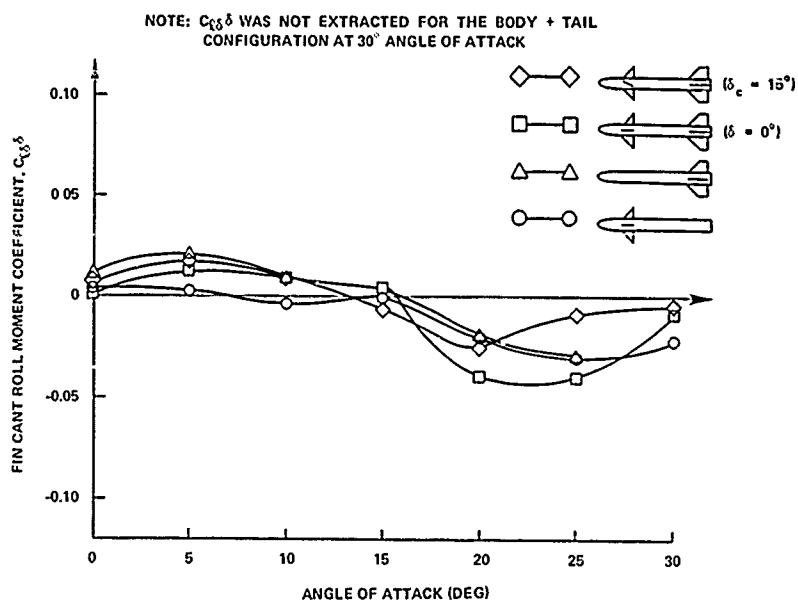


Figure 23. Extracted Fin Cant Roll Moment Coefficients vs Angle of Attack for Canard Controlled Missile Configurations

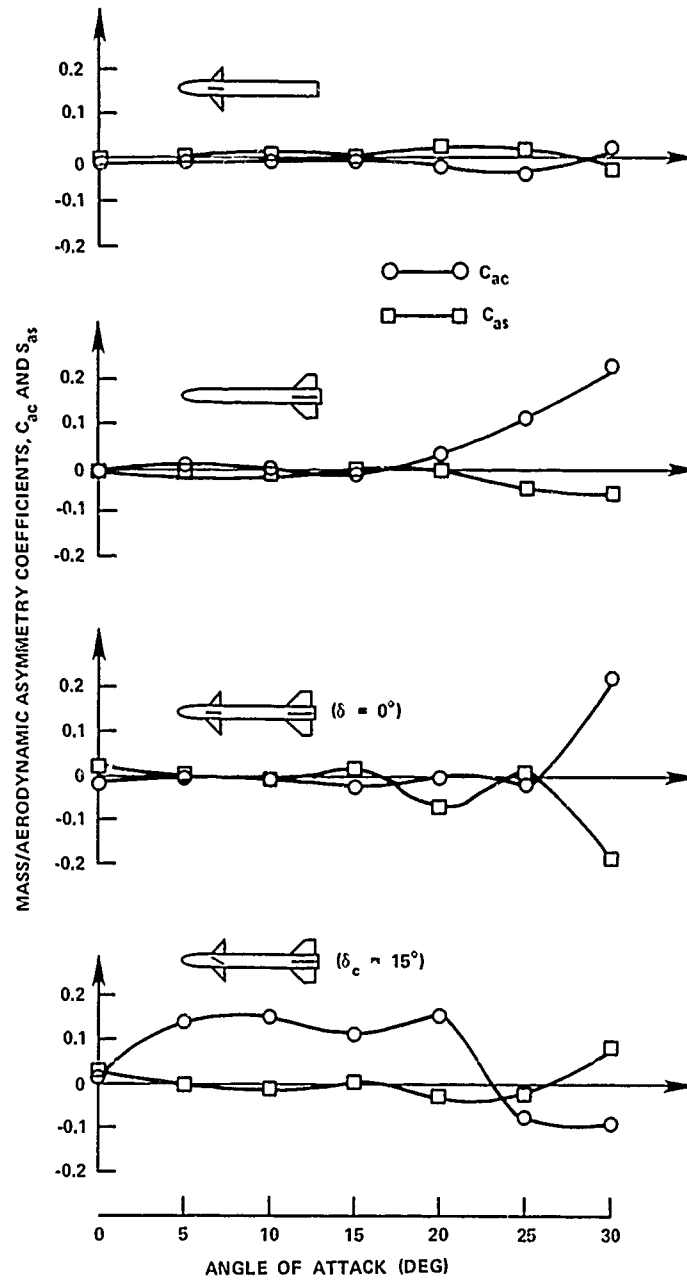


Figure 24. Extracted Mass/Aerodynamic Roll Moment Asymmetry Coefficients vs Angle of Attack for Canard Controlled Missile Configurations

It is important to note that $C_{\dot{r}P(4\gamma)}$ is required in addition to $C_{\dot{r}P}$ to model the roll damping characteristics of the configurations, especially at the higher angles of attack due to positive roll damping moments. The dependence of the roll motion on $C_{\dot{r}P(4\gamma)}$ manifests itself in roll oscillations that initially shrink but do not damp. The configurations with tail fins exhibit this phenomenon.

The extracted linear damping coefficient ($C_{\dot{r}P}$) is nonlinear with angle of attack for the configurations with tails. The canard contribution to the canard + body + tail total roll damping moment is nearly cancelled by canard/tail interference. It has been shown that theoretical estimates of canard + body + tail $C_{\dot{r}P}$ provided by the Naval Weapons Center,²⁴ China Lake agree with the experimental results at angles of attack up to 20° . The 15° canard pitch deflection increases the negative roll damping moment at angles of attack above 15° .

The extracted induced roll moment coefficients ($C_{\dot{r}(4\gamma)}$) show that the canard contribution to the total induced roll moment of the canard + body + tail configuration is small. The fin cant moment coefficients are small since there was no intentional fin cant.

Extracted mass/aerodynamic asymmetry coefficients showed some unusual results for the configurations that have tails. The canard + body configuration exhibited small asymmetry coefficients at all angles of attack as expected. However, the configurations with tails exhibited large aerodynamic asymmetries on symmetric configurations at the higher angles of attack. Purely mass asymmetries would have been small and constant with respect to angle of attack. The canard + body + tail configuration with the 15° canard pitch deflection was expected to exhibit an aerodynamic asymmetry due to the deflected canards.

Although the three applications of the fitting technique were successful, several problems were encountered. The technique is still time consuming and expensive. In future efforts, Kalman filtering and increased automation should be applied to streamline the process. All of the wind tunnel tests conducted, thus far, have been at low speeds because the air bearing is load-limited. In order to extract aerodynamic roll coefficients at high speeds, new transonic and supersonic test equipment is required.

PASSIVE ROLL RATE STABILIZATION

The dynamic stability of free-flight, fin-stabilized ordnance is critically dependent on roll rate, as shown in Figure 25. If the roll rate is too low, the weapon may develop catastrophic yaw or resonance instability. Magnus instability may occur when the roll rate is large at high angles of attack. Theoretically, there is a region of spin rates where the missile could sustain dynamic stability. This ideal roll rate is above the resonance frequency and below the roll rate required for Magnus instability. Consequently, this ideal roll rate cannot be sustained over the operational angle of attack range due to the nonlinear nature of the roll rate characteristics of conventional fins.

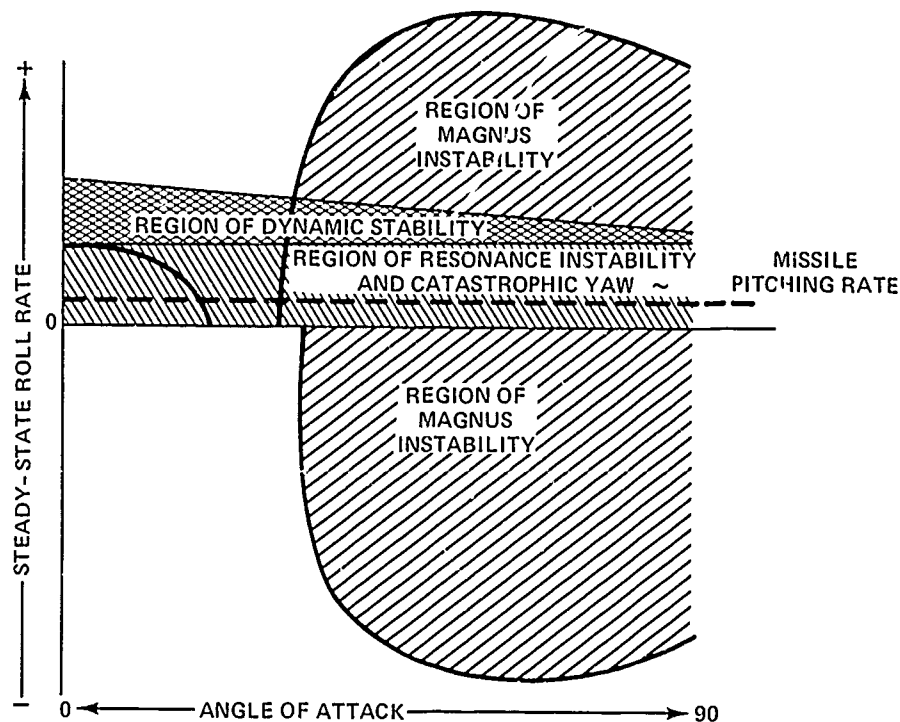


Figure 25. Roll Rate vs Dynamic Stability for a Four Fin Missile

In 1961 H. Lugt²⁵ suggested that slots or gaps in the fin planform might radically alter the dynamic angular motion of finned bodies by sweeping away strong wake vortices attached to the receding fin at very large angles of attack. Lugt made this suggestion based on his observation that an autorotating sliver of paper could be roll rate stabilized by a near full span slot.

Pursuing the possibility that the mechanism of roll speed up was related to flat plate autorotation led to an experiment conducted in 1966²⁶ that showed that the roll rate of a cruciform fin system could be significantly reduced at high angles of attack by slots. Figure 26 is a schematic of the free rolling cruciform fin systems tested. Figure 27 shows the effect of slots on steady state roll rate and roll lock in angle.

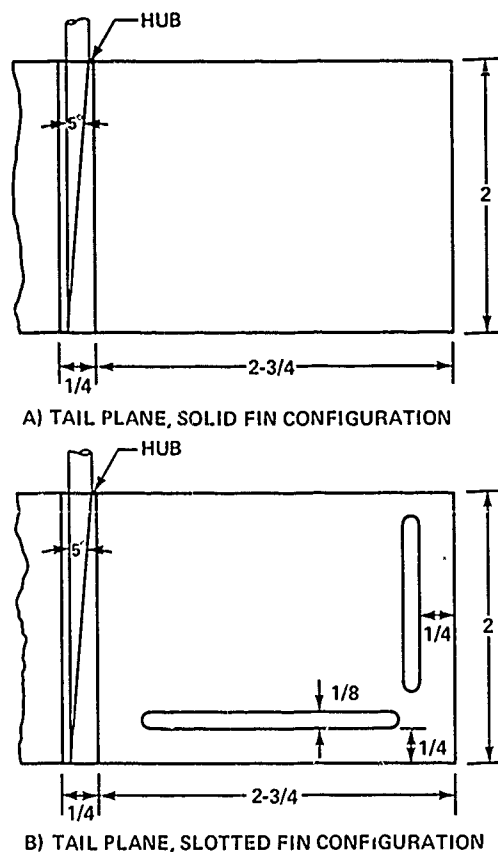


Figure 26. Schematic of Free-Spinning Cruciform Fins
(Dimensions in Inches)

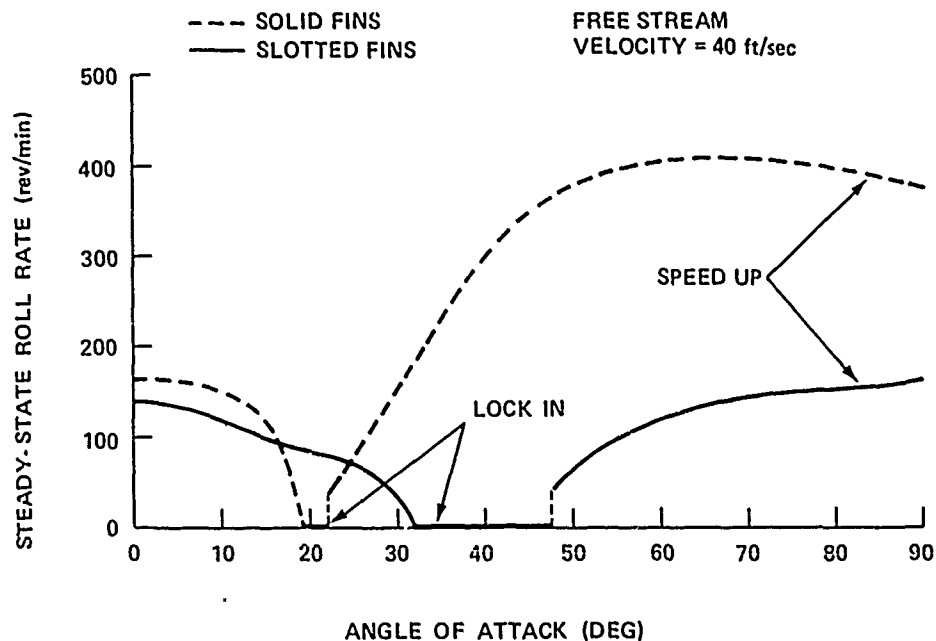


Figure 27. Rotational Characteristics of Cruciform Rectangular Fins

It was further suggested that this fin addition could be used to reduce the possibility of Magnus instability and catastrophic yaw.

In later research,²⁷ subsonic wind tunnel tests were conducted at the Naval Academy to determine the effect of slot size on the longitudinal stability and rolling characteristics of a cruciform finned missile. The tests were conducted at approximately 150 ft/sec. The test specimen is shown in Figure 28.

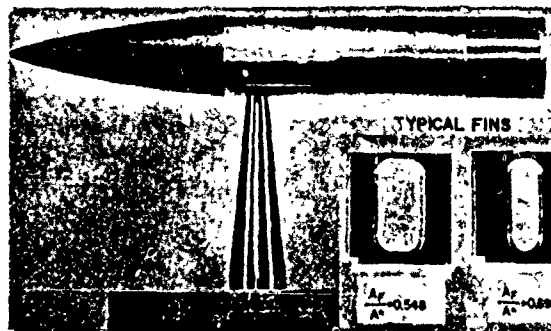


Figure 28. Wind Tunnel Model (Naval Academy)

The Naval Academy model had a 3.2-caliber ogive nose with a 4.4-caliber cylindrical afterbody. The model's maximum body diam. was 1.5 in. The fins were rectangular and trapezoidal, with an exposed semispan of 1 caliber.

A free-rolling test was conducted to determine the effect of fin slots and fin cant on roll lock in and roll speed up.

Figure 29 gives the steady-state spin rate vs angle of attack for the Naval Academy model with solid rectangular fins and approximately no fin cant.

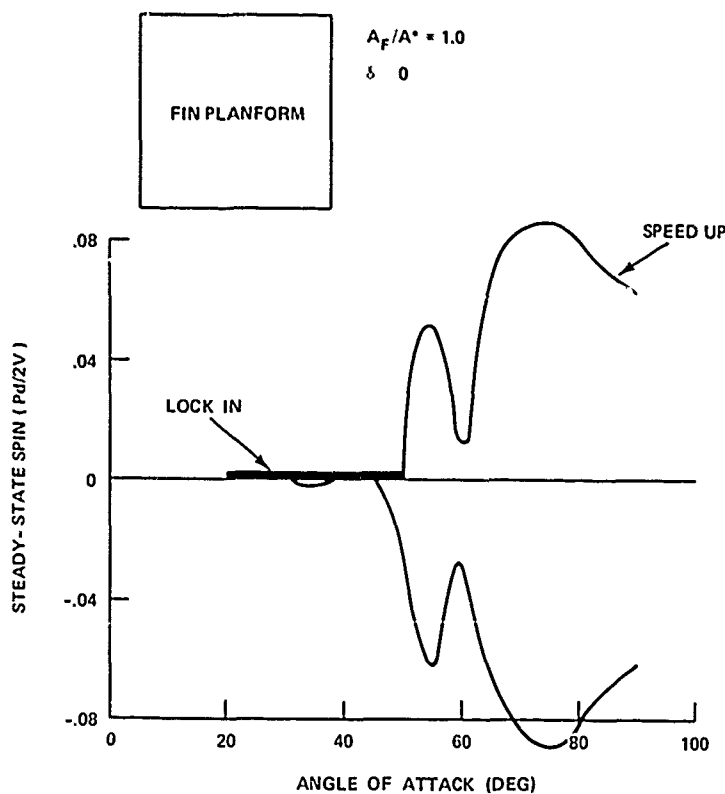


Figure 29. Steady-State Rolling Velocity vs Angle of Attack for Naval Academy Model With Solid Rectangular Fins. Fin Cant 0.

Lock-in exists from 20° to 50° angle of attack. Considerable speed up exists above 50°. Dual modes of motion exist throughout. Very slow clockwise motion existed below 20° and was not recorded. The fin cant was then varied from zero to a maximum of 8° in order to overcome the lock in.

Figure 30 gives the steady state roll rate vs angle of attack for the Naval Academy model with solid rectangular fins and 8° of fin cant. Lock in now occurs at 30° rather than at 20° , which is generally beneficial. The speed up is hardly affected. Not only is the spin high at high angles of attack but it is also independent of the fin cant.

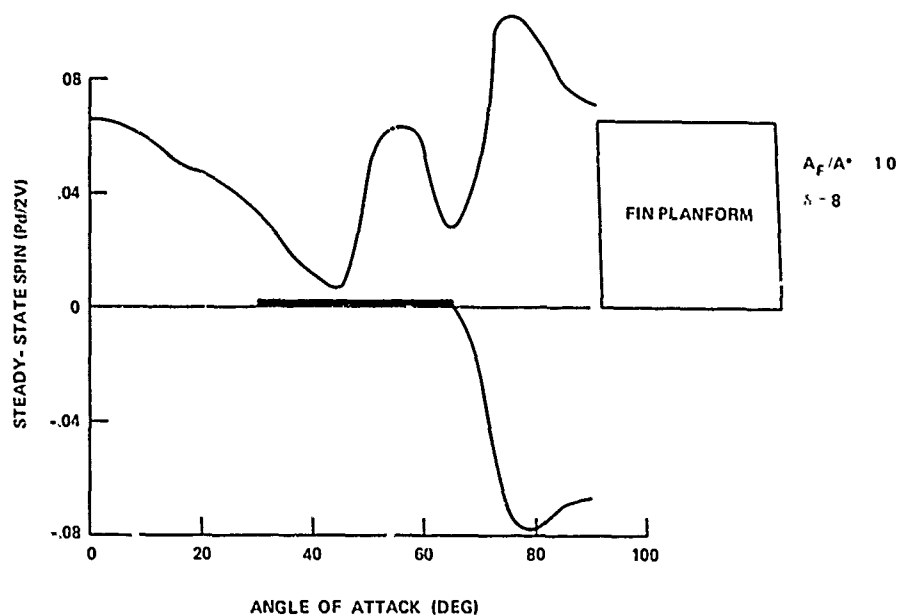


Figure 30. Steady-State Rolling Velocity vs Angle of Attack for Naval Academy Model With Solid Rectangular Fins. Fin Cant 8° .

These results are typical for conventional cruciform fin systems. The motion of the Naval Academy model was then investigated with varying slot size and fin cant.

The addition of the slot eliminates roll speed up if the slot is sufficiently large. Figure 31 gives the motion for the minimum slot size which alleviated roll speed up for the rectangular fin configuration. Fin cant is nearly zero. Some slight residue of speed up exists. However, with the addition of cant as shown in Figure 32, no speed up is apparent. The spin is higher at low angles of attack. However, it is only $\frac{3}{4}$ of the maximum spin of an uncanted solid fin, and the maximum spin of the slotted fin occurs at the smallest angle of attack where it is least critical. The minimum lock in angle is now moved up to 35° . There is still the possibility of lock in but only if the missile's rolling motion is stopped. It should also be noted that the roll damping for this configuration is stabilizing: $L(\dot{\gamma}) < 0$ for all positive

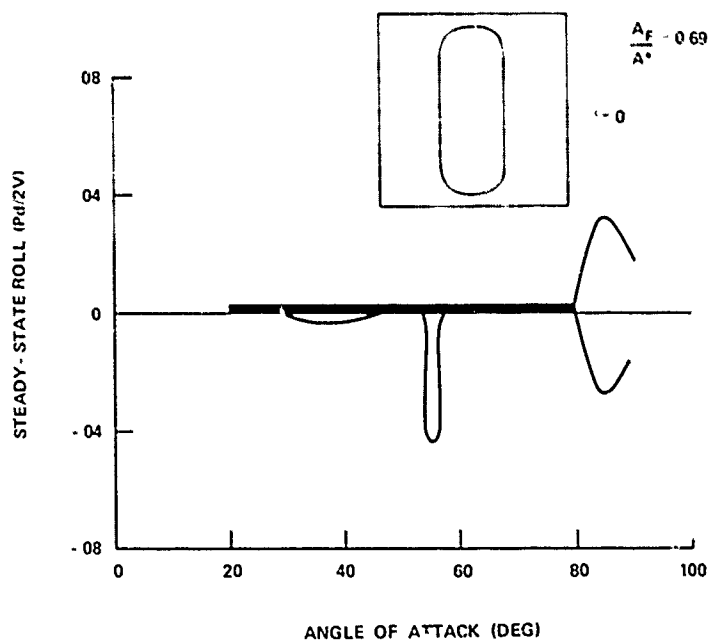


Figure 31. Steady-State Rolling Velocity vs Angle of Attack for Naval Academy Model With Rectangular Fins and a Slot $A_F/A^* = 0.691$, $\delta = 0^\circ$.

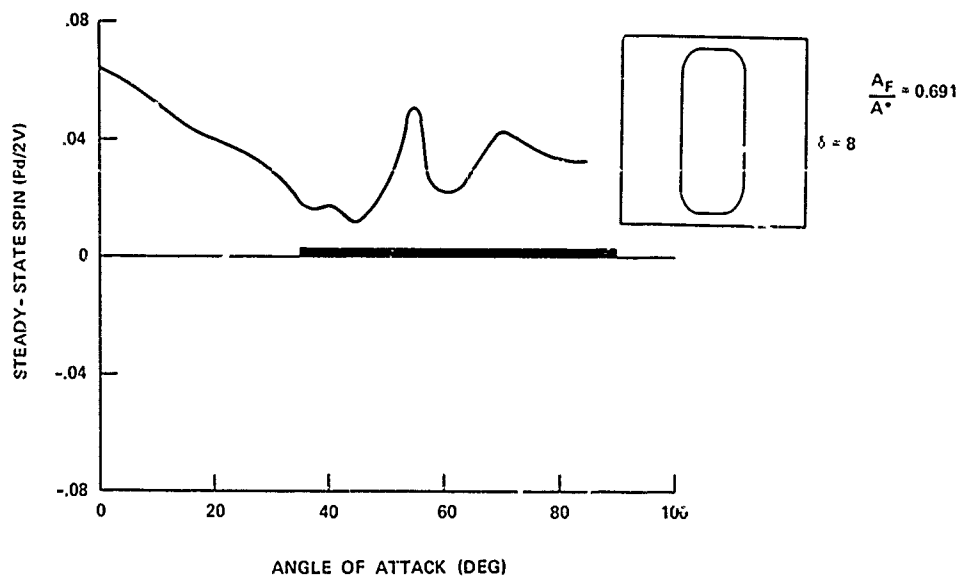


Figure 32. Steady-State Rolling Velocity vs Angle of Attack for Naval Academy Model With Rectangular Fins and a Small Slot. $A_F/A^* = 0.691$, $\delta = 8^\circ$.

values of $\dot{\gamma}$. Above an angle of attack of 35° the missile will spin. If we reduce its spin below a critical value, it will damp. This phenomenon can occur only if the roll damping torque is negative for positive spin rates. Conversely, roll speed up¹⁵ of the solid fin configuration can occur only if the roll damping is destabilizing.

It was obvious that the ratio of induced rolling moment to fin cant moment was improved. From the response of the model, it was felt that even a slight change in the ratio might eliminate the lock in mode. Possibly a higher fin cant or more efficient slot shape could have eliminated it. A larger fin cant could not be tested due to the limits of the model design.

Figure 33 shows that a slightly smaller slot nearly eliminates the lock-in mode. However, speed up is present, even though considerably weakened.

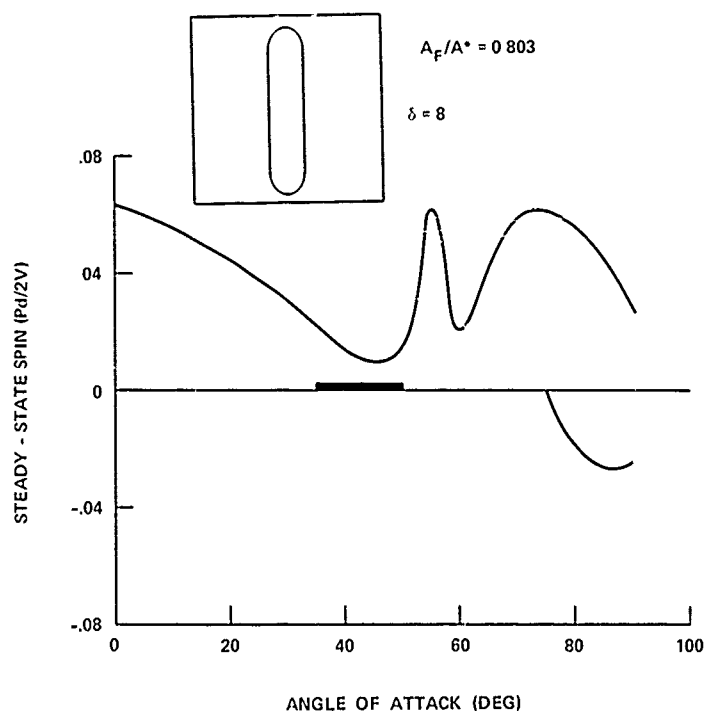


Figure 33. Steady-State Rolling Velocity vs Angle of Attack for Naval Academy Model With Rectangular Fins and a Small Slot.
 $A_F/A^* = 0.803$.

During the Naval Academy tests, both rectangular and trapezoidal fins were studied. The results obtained were essentially the same for both types of fins.

Single degree of freedom, free oscillation tests were then conducted at the Naval Academy to determine the effect on the missile's longitudinal stability due to slot size.²⁸ Pitching motion was recorded and these data were fit using a nonlinear, least squares technique. Both the linear and nonlinear contributions of the restoring moment and pitch damping moment were determined. The results of this study indicated that the slot reduces longitudinal static stability at low angles of attack but increases it at high angles of attack. Only with extreme slot size ($A_F/A^* \leq 0.347$) was the model statically unstable. No dynamic instability was present.

Returning to Figure 31, one might conclude that the slot itself, without the presence of fin cant, actually promotes lock in. Returning to Figure 32, we note that this is not the case at the moderate angles of attack because the minimum lock in angle is greater.

In order to determine if the slot promoted lock in at higher angles of attack, a test was conducted at NSRDC to study the effect of slot size on the induced rolling moment. The basic finner was used as the test specimen because of its availability. Fins identical to those tested at the Naval Academy were studied.

The effect of slot size on the induced roll moment is presented in Figures 34 and 35. At an angle of attack of 45° (Figure 34), the slot significantly reduces the induced rolling moment. The effect of slot size on the induced rolling moment at higher angles of attack is equally dramatic. Figure 35 summarizes the results of the test. It is noted that the induced rolling moment was reduced by as much as 70% for the slot sizes tested and the small slot is nearly as efficient as the large slot in reducing the induced rolling moment.

Based on the results of these wind tunnel studies, it was concluded that, at subsonic speeds, the slotted fin is superior to the solid fin in that it eliminates roll speed up, appreciably reduces the induced rolling moment, and increases longitudinal stability at high angles of attack. Stability is reduced at low angles of attack. However, it would appear from the data that the possibility of catastrophic yaw is minimized.

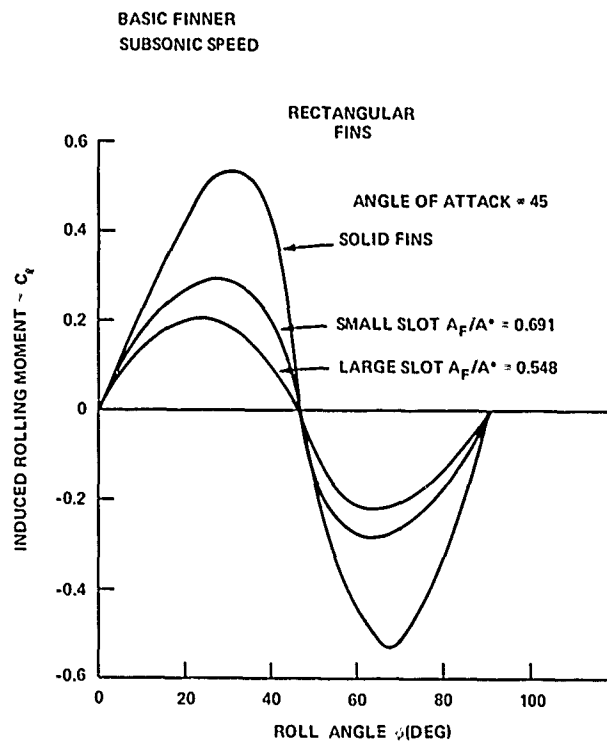


Figure 34. Typical Effect of Slot on Induced Rolling Moment

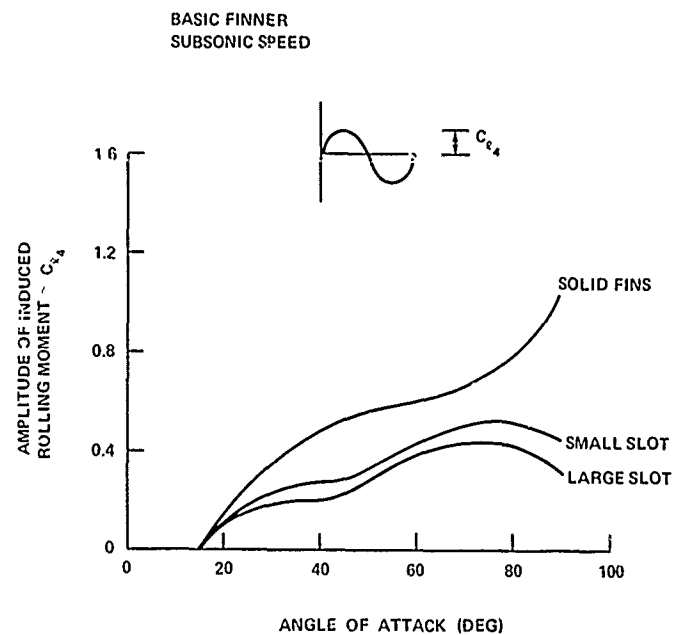


Figure 35. Effect of Slot on Amplitude of Induced Rolling Moment

ROLL RATE STABILIZED LOW DRAG BOMB

The Navy's MK 81 Low Drag Bomb has always suffered from marginal dynamic stability characteristics.⁴ At least one in ten of these bombs falls short due to excessive yawing motion produced by roll lock in. Consequently, it was felt that this configuration (shown in Figure 36) would be an ideal research configuration for studying the effect of roll rate stabilization. Therefore, free rolling and free pitching tests²⁹ were conducted on a full-scale MK 81 Low Drag Bomb in the NSRDC 8- X 10-ft subsonic wind tunnel.

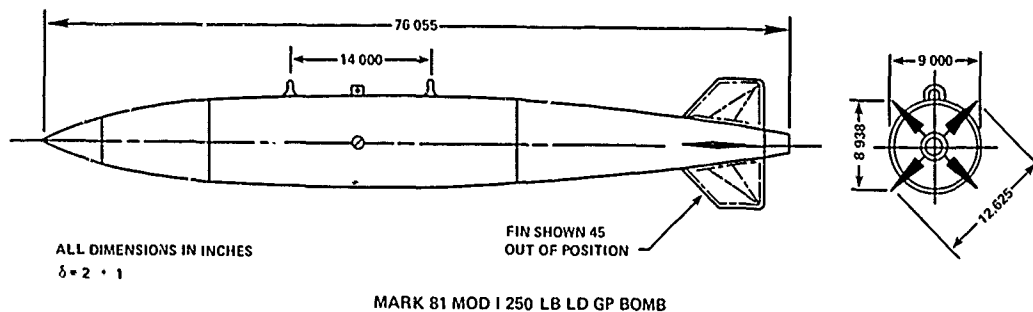


Figure 36. Schematic of the MK 81 Low Drag Bomb

Optimum slot size and location were determined from free rolling tests through the use of interchangeable fin inserts. Aileron tabs on the fin trailing edges were employed to avoid roll lock in. Dynamic free pitching tests showed a slight loss in restoring moment for the bomb with fin slot and aileron tab modification. The pitch damping rate was virtually unchanged.

Initially, ten bombs were dropped from an altitude of 30,000 ft with an air speed of 350 kn at the White Sands Missile Range. It is estimated that their steady state roll rates varied between 30 and 60 rev/sec. Test data indicated that all bombs flew well. The circular error probability (CEP), the estimated radius of a circle that encompasses 50% of the total population of the bombs (excluding any initial disturbance caused by aircraft separation effects) was 56 ft, or 1.54 mil in the plane normal to the trajectory at impact.

Although it appeared that the slots and tabs had improved the MK 81's flight performance, it was felt that the sample size was too small. Moreover, the bombs were ejected with a normal, and consequently small, launch disturbance. It was felt that a more rigorous test might be in order.

A second flight test was initiated³⁰ at the White Sands Missile Range where standard MK 81 bombs were compared directly to the modified version. Thirty-one standard bombs and twenty-seven slotted fin bombs with aileron tabs were dropped. Three different release conditions were investigated. The bombs were ejected with intentionally large pitch rates in order to properly evaluate their stability. In all cases, the bombs experienced a first maximum pitch of between 60 and 90°. Four different aircraft (A-4F, A-7E, A-4E, A-7A) and two different racks (MAU 9/A, AERO 7A) were used in the test. However, the large initial yaw experienced by all bombs made these differences negligible.

The flight conditions that were investigated are presented in Table 2. Only six drops of the modified configuration were made at a release condition of 30,000 ft and 350 kn. However, ten modified bombs had been previously dropped at this condition with a lower initial launch disturbance and flew well.²⁹ Consequently, it was felt that a smaller sample of drops was sufficient for this condition.

Table 2. Flight Conditions and Test Drops for the Standard Low-Drag Bomb and Modified Configuration

<u>Release Conditions</u>		<u>Test Specimens (No. of Drops)</u>	
<u>Altitude (ft)</u>	<u>Velocity (kn)</u>	<u>Standard Configuration</u>	<u>Modified Configuration</u>
30,000	350	10	6
20,000	500	8	10
20,000	300	13	11

Films from the flight program showing the detailed release and yawing motion of the stores, were analyzed. These films revealed that four standard configurations developed instabilities (yaw grows in magnitude with time) of the roll-yaw coupling type. In all of these cases, the spin was nearly equal to the nutation frequency during the unstable portion of the trajectory. Two flights were extremely bad in that these bombs developed a nearly "flat spin" which in one case lasted from launch to impact. The other bombs damped only a few seconds before impact.

All modified configurations appeared to be stable (the yawing motion does not grow in magnitude with time). However, four drops were slow to damp the launch disturbance. (One drop required 25 sec (22 cycles) for the yaw to damp (an extremely bad flight). Three drops required 10 cycles of yaw or less to damp.)

It was concluded that the slot-tab modification had significantly improved the flight performance of the MK 81 bomb. It was also felt that optimizing the tab angle would result in even further improvement of the dynamic stability characteristics.

It should also be noted that further tests conducted by the Air Force using the MK 82 bomb (500-lb) with identical tabs but without slots resulted in a large number of severely unstable flights due to Magnus instability. However, these results remain unpublished.

PRACTICAL APPLICATION

The MK 82/BSU-49B, as shown in Figure 37, is being developed jointly by the Air Force and Navy as a replacement for the MK 82 Low Drag Bomb and the MK 82/SNAKEYE retarded bomb. This new dual mode bomb is stabilized in the unretarded mode by slotted fins (see Figure 38).

Figures 39 through 41 present some of the aerodynamic stability characteristics of this particular weapon as obtained from wind-tunnel tests.³¹ Figure 39 shows the low speed roll rate characteristics of this vehicle with solid fins as obtained from single-degree-of-freedom, free rolling tests. At high angles of attack, the roll rates are extreme. However, by appropriate slotting and adding turning wedges, the roll rate can be tailored to alleviate roll-yaw coupling instabilities, as shown in Figure 40.

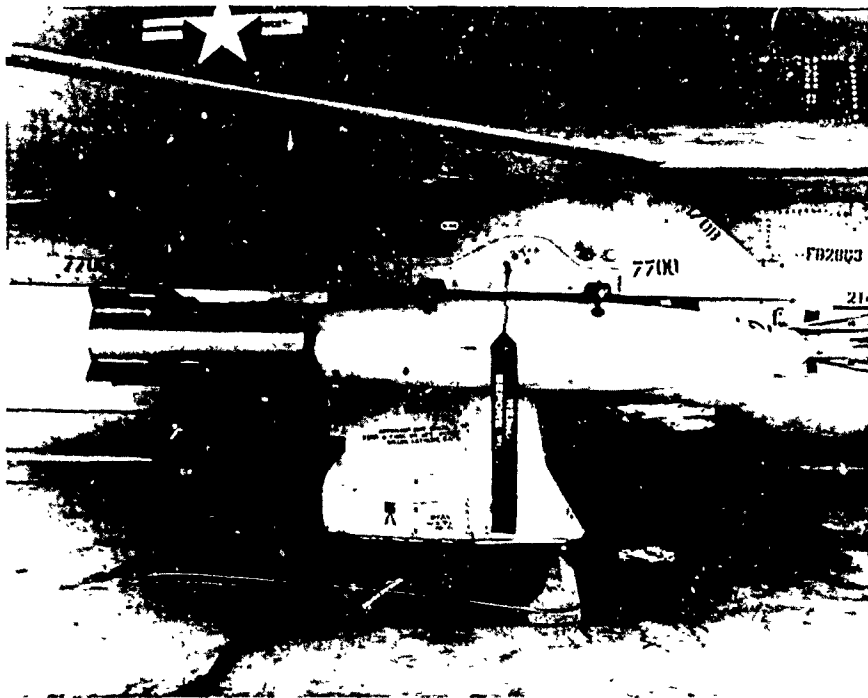
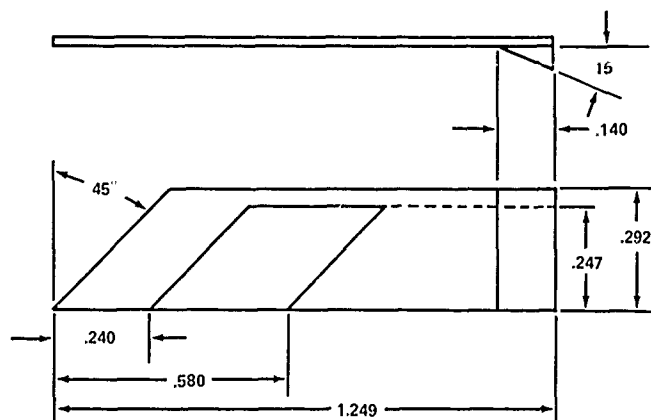


Figure 37. WSMR Test Vehicle (MARK 82/BSU-49B)

FIN PLANFORM



ALL DIMENSIONS IN CALIBERS

Figure 38. BSU-49B Fin Planform

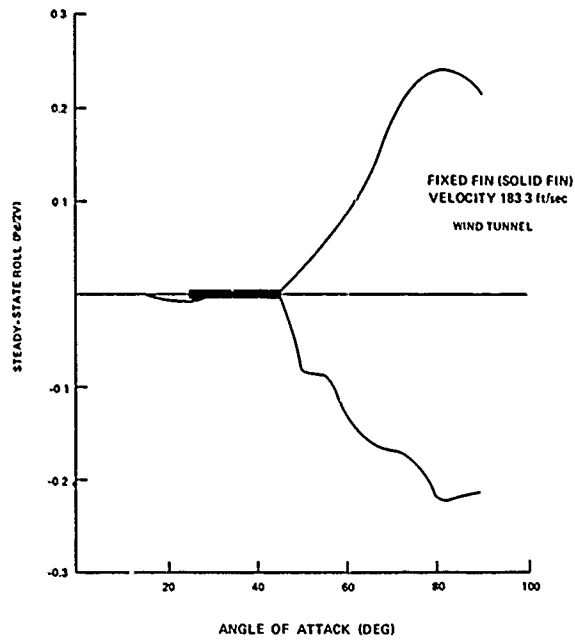


Figure 39. Free Rolling Characteristics of Solid Fin Vehicle

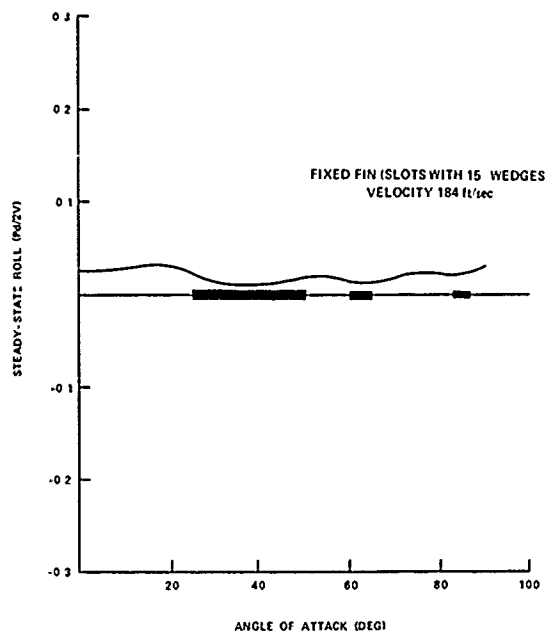


Figure 40. Free Rolling Characteristics of Slotted Fin Vehicle

The effects on stability derivatives; $C_{z\alpha}$, $C_{m\alpha}$, and $C_{m_q} + C_{m_{\dot{\alpha}}}$ are shown in Figure 41 and are also compared with the Navy Low Drag Bomb. The normal force derivatives ($C_{z\alpha}$) of the three configurations are comparable, and the restoring moment of the low drag bomb is considerably greater. However, the BSU-49B with slots has considerably more damping.

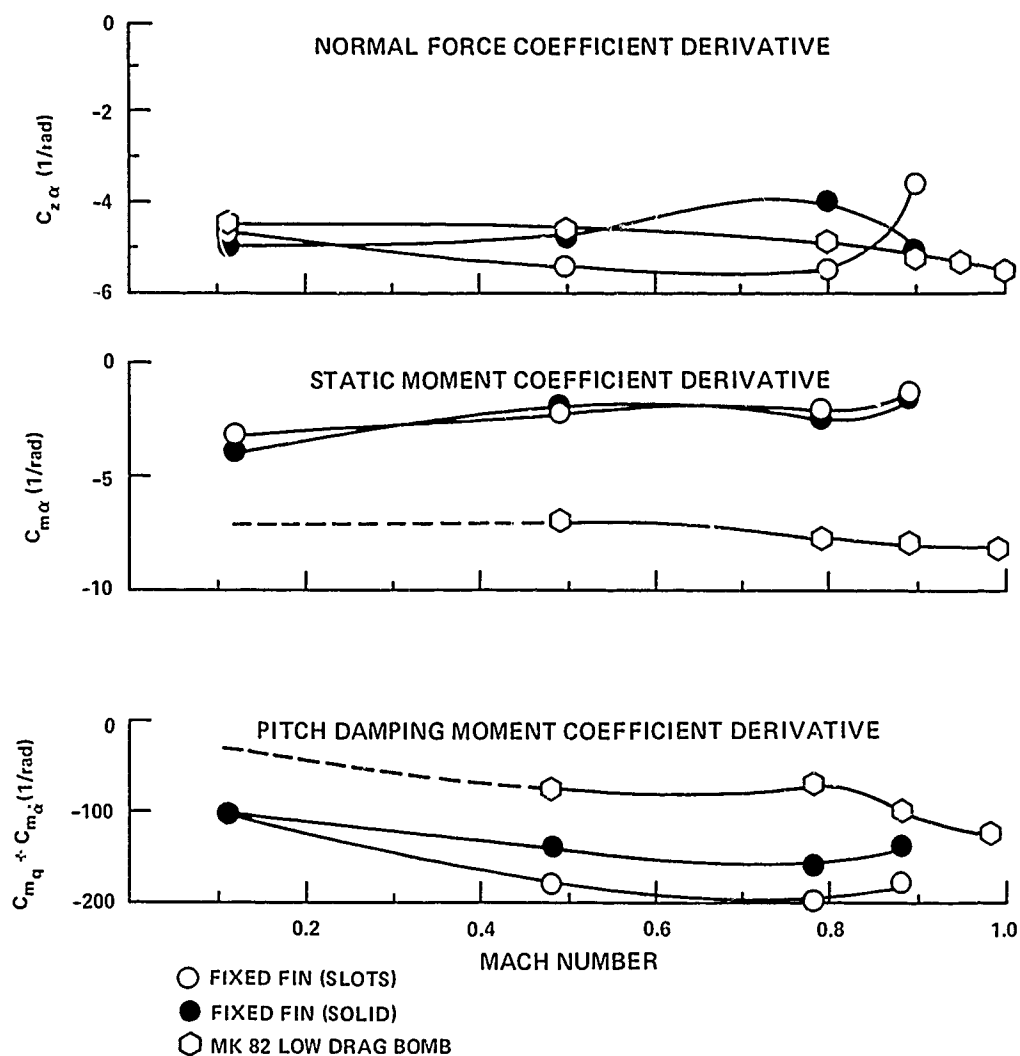


Figure 41. Effects of Fin Configuration on Stability

Flight tests³² of the MK 82/BSU-49B showed that "fine tuning" of the roll rate could result in considerably improved dynamic stability. Figure 42 shows the release envelope and dynamic stability characteristics of the MK 82/BSU-49B for 19 bombs with 10° wedges launched with an intentionally large launch disturbance ($50^\circ < \alpha_{max} < 75^\circ$) and a Mach number range of $0.4 \leq M \leq 1.35$. Most (94.5%) of the stores were dynamically acceptable, e.g., the time to damp was small compared to the time of flight. Bombs with 15° wedges developed Magnus instability at low speed ($M = 0.4$).

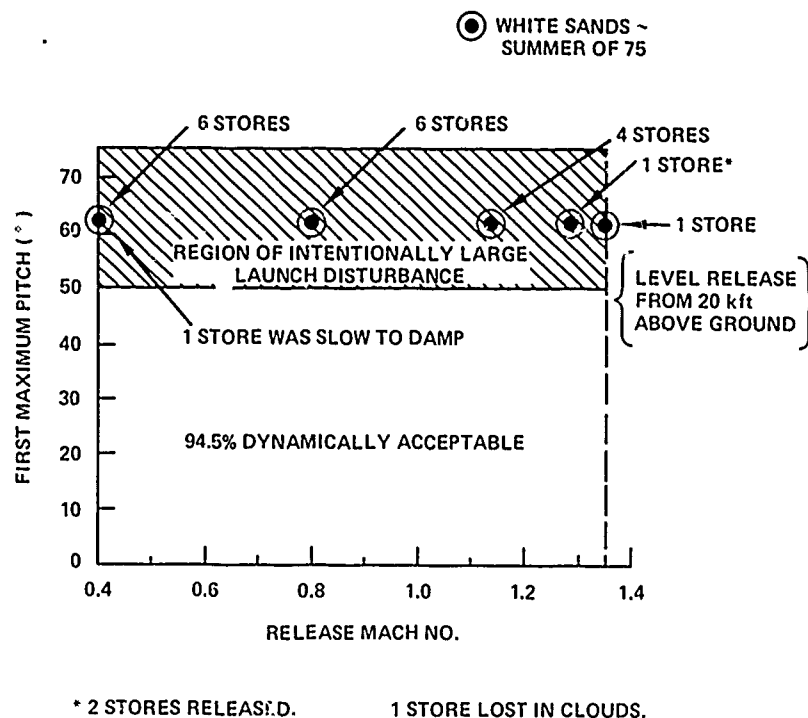


Figure 42. Release Envelope and Dynamic Stability Characteristics
(WSMR Test Vehicle With 10° Turning Wedges)

Later flight tests, on a modified configuration, showed that fin and forebody configuration modifications somewhat degraded the flight characteristics. However, all instabilities noted were slightly outside of the bomb's normal operational envelope.³²

CONCLUSIONS

1. The single-degree-of-freedom roll motion of finned missiles can now be modeled accurately at high angles of attack through the use of a more complex representation of the static and dynamic roll torques.
2. Roll rate stabilization by fin slots can be an effective method of alleviating roll-yaw coupling instabilities.

REFERENCES

1. J. D. Nicolaides, *Missile Flight and Astrodynamics*, Bureau of Naval Weapons, TN 100-A, Washington, D.C., 1959-1961.
2. J. D. Nicolaides, *On Missile Flight Dynamics*, Dissertation, The Catholic University of America, School of Engineering and Architecture, Washington, D.C., 1963.
3. J. D. Nicolaides, *On the Free Flight Motion of Missiles Having Slight Configurational Asymmetries*, Ballistic Research Laboratory BRL Report No. 858, 1953, and IAS Preprint No. 395, Aberdeen, Maryland, 1952.
4. C. H. Wingo, Jr. and F. L. Jones, *Free Flight Catapult Tests of 250-Lb Low Drag GP Bomb, Type EX-2 MOD 2, EX-2A, 250-Lb Low Fragmentation Bomb, Type EX-17, MOD 6, 2000-Lb Low Drag GP Bomb, Type EX-11, MOD 1 With Canted Fins*, Naval Proving Ground, Report 1419, Dahlgren, Virginia, October 1955.
5. R. H. Heald, H. Crouch, and G. H. Adams, NBS Report No. 5156, February 15, 1957.

6. J. D. Nicolaides and T. F. Griffin, *On a Fluid Mechanism for Roll Lock-In and Rolling Speed-Up Due to Angle of Attack of Cruciform Configurations*, Bureau of Ordnance, BTN 16, Washington, D.C., 1955.
7. J. D. Nicolaides, *On the Rolling Motion of Missiles*, Bureau of Ordnance BTN 33, Washington, D.C., 1957.
8. L. Bairstow, B. M. Jones, and B. A. Thompson, *Investigation Into the Stability of an Aëroplane*, Br. ARC R and M 77, 1913.
9. L. Bairstow, *Applied Aerodynamics*, 1920.
10. E. B. Kasari and R. W. Bratt, Douglas Aircraft Company, Report ES 17254, 1953.
11. E. Schneller, *On the Wobbling Motion of an Arrow Stable Body in Free Flight*, Translation by N. S. Medoedeff, Goodyear Aircraft Corporation.
12. J. C. Crown and S. Fagin, *Some Non-Linear Aspects of Missile Motion*, Unpublished NOL paper.
13. J. D. Nicolaides, *An Hypothesis for Catastrophic Yaw*, Bureau of Ordnance Ballistic Technical Note No. 18, Washington, D.C., September 1955.
14. C. J. Cohen and D. Werner, *A Formulation of the Equations of Motion of a Four-Finned Missile*, Naval Ordnance Systems Report 5133, Washington, D.C., September 27, 1956.
15. Peter Daniels, "A Study of the Nonlinear Rolling Motion of a Four-Finned Missile," *Journal of Spacecraft and Rockets*, Vol. 7, No. 4, April 1970, pp. 510-512.
16. F. L. Stevens, *Subsonic Wind Tunnel Tests of the Basic Finner Missile in Pure Rolling Motion*, Naval Weapons Laboratory Technical Note TN-K-4/72, Dahlgren, Virginia, February 1972.
17. C. J. Cohen and T. A. Clare, *Analysis of the Rolling Motion of Finned Missiles at Large Angles of Attack*, Naval Weapons Laboratory Technical Report TR-2671, Dahlgren, Virginia, February 1972.

18. C. J. Cohen, T. A. Clare, and F. L. Stevens, *Analysis of the Nonlinear Rolling Motion of Finned Missiles*, AIAA Paper No. 72-980, Palo Alto, California, 1972.
19. J. H. Reynolds, *ROMOF a CDC 6700 Computer Program for Fitting Rolling Motion Data of Cruciform-Finned Missiles*, Naval Weapons Laboratory Technical Note TN-K-42/76, Dahlgren, Virginia, July 1973.
20. S. R. Hardy, *Nonlinear Analysis of the Rolling Motion of a Wrap-Around Fin Missile at Angles of Attack from 0 to 90° in Incompressible Flow*, Naval Surface Weapons Center/Dahlgren Laboratory Technical Report TR-3727, Dahlgren, Virginia, September 1977.
21. Peter Daniels and S. R. Hardy, "Roll Rate Stabilization of a Missile Configuration With Wrap-Around Fins," *Journal of Spacecraft and Rockets*, Vol. 13, No. 7 of July 1976, pp. 446-448.
22. S. R. Hardy, *Subsonic Wind Tunnel Tests of a Canard-Control Missile Configuration in Pure Rolling Motion*, Naval Surface Weapons Center/Dahlgren Laboratory Technical Report TR-3615, Dahlgren, Virginia, June 1977.
23. S. R. Hardy, *Nonlinear Rolling Motion Analysis of a Canard-Controlled Missile Configuration at Angles of Attack from 0 to 30° in Incompressible Flow*, Naval Surface Weapons Center/Dahlgren Laboratory Technical Report, Dahlgren, Virginia, to be published.
24. R. E. Meeker, "Roll Damping Studies Progress Report for FY 1976 and 1976 TQ," Naval Weapons Center Technical Memorandum 2929, China Lake, California, October 1976.
25. H. J. Lugt, "Self-Sustained Spinning of a Cruciform Fin System," *Proceedings of the Fifth United States Navy Symposium on Aeroballistics*, Naval Ordnance Laboratory, White Oak, Maryland, 1961.
26. P. Daniels, "Fin Slots vs Roll Lock In and Roll Speed Up," *Journal of Spacecraft and Rockets*, Vol. 4, No. 3, March 1967, pp. 410-412.
27. P. Daniels and T. A. Clare, "Aerodynamic Characteristics of the Slotted Fin," *Journal of Aircraft*, Vol. 9, No. 8, August 1972, pp. 603-605.
23. T. A. Clare and P. Daniels, *Effect of Fin Slots on the Static and Dynamic Stability Characteristics of Finned Bodies*, Naval Weapons Laboratory Technical Report TR-2582, Dahlgren, Virginia, June 1971.

29. P. Daniels, "Effect of Fin Slots and Fin Tabs on the Dynamic Stability Characteristics of the Navy Low Drag Bomb," *Journal of Spacecraft and Rockets*, Vol. 7, No. 9, September 1970, pp. 1151-1152.
30. P. Daniels, *A Comparison of the Stability Characteristics of Standard Fin and Slotted Fin MK 81 Low Drag Bombs*, Naval Weapons Laboratory Technical Report TR-2722, Dahlgren, Virginia, April 1973.
31. Naval Surface Weapons Center, "Air Inflatable Retarder Preliminary Wind-Tunnel Test Results and Recommendations," ltr KBC:JHR:mhl, Dahlgren, Virginia, 1 April 1975.
32. P. Daniels and John Sun, *Development Flight Tests of the Low-Drag BSU-49B Air Inflatable Retarder*, NSWC/DL Technical Report TR-3579, Naval Surface Weapons Center/Dahlgren Laboratory, Dahlgren, Virginia, April 1977.
33. P. Daniels, "A Flow Visualization Study of Free Rolling Cruciform Fins in Cross Flow," Naval Weapons Laboratory Technical Report TR-3053, Dahlgren, Virginia, November 1973.